

institute for optical systems
annual report 2016

Foreword

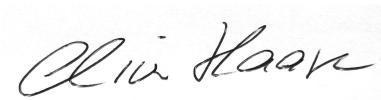


Hochschule Konstanz University of Applied Sciences (HTWG) has been one of the first Universities of Applied Sciences that has clearly committed itself to applied research. Today, HTWG has positioned itself in the growing group of research active Universities of Applied Sciences, and is continuously striving for even greater excellence, visibility, and leadership.

The research institutes play an essential role in the overall research activities of HTWG. The Institute for Optical Systems (IOS) has been founded as one of three focus institutes in 2008, and has lived up to its mission and HTWG's expectation ever since.

Measuring the success of research is generally a difficult task. It becomes easy, however, for individuals and institutes alike that contribute to the scientific community in many different ways. The IOS clearly is such an institute. Its members have published their work in numerous high quality publications, they have acquired substantial amounts of external funding, and they have successfully led several doctoral candidates to their advanced degree, to name only the most obvious contributions. The institute's success has only been possible because of the enthusiasm of its members, and its tight integration with HTWG. Students have contributed to the research work on various levels, and the results have been fed into the members' teaching. In this sense, the IOS has demonstrated the importance of excellent applied research also as a means for high quality teaching, in particular on the graduate level.

I am proud to write these few lines of thanks and congratulations for the IOS and cordially wish the institute, but first and foremost its members, ongoing enthusiasm, thirst for knowledge, and success for the future.

A handwritten signature in black ink that reads "Oliver Haase". The signature is written in a cursive, flowing style.

Prof. Dr. Oliver Haase
Vice-President for Research, University of Applied Sciences Konstanz

Preface

The present report gives an overview over the research and development activities of the Institute for Optical Systems (IOS) Konstanz in the year 2016. Our main fields of interest are cognitive systems, geometric modelling, image processing, optical metrology and light engineering, thus representing the fundamental disciplines of current optical technology. The focus on optical systems as a whole allows us to offer competent partnership to the local industry in all relevant aspects. The IOS was founded in April 2008 by four professors from three different faculties of the University of Applied Sciences at Konstanz and is led by Prof. Dr. Umlauf (director) and Prof. Dr. Franz (associate director).

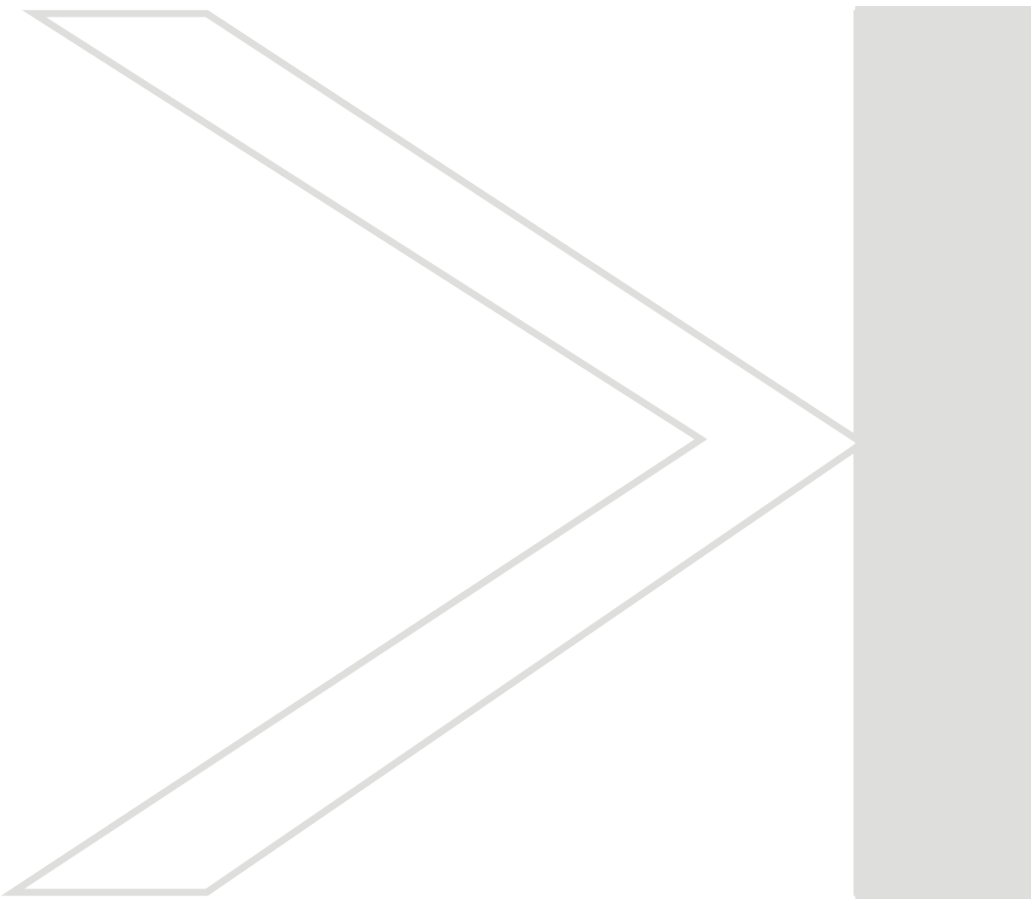
The following project descriptions present ongoing activities mainly on a status report level. Most of the reports are written by students working on their diploma, bachelor, master or Ph.D. theses. They reflect the largely varying levels of content, practice and insight that are characteristic for an institution involved in academic education. Due to its interdisciplinary nature, research at the IOS combines approaches from optics, computer graphics, image and signal processing, metrology, light engineering and sensor technology typically resulting in optical systems on a prototype level, either in pre-phase research or in cooperation with local industry.

On the occasion of our annual report, we would like to thank all of our students and co-workers for their enthusiasm and dedication which makes our institute a great place to be. Special thanks go to our institute officers, Pascal Laube, Martin Schall and Michael Grunwald for smoothly managing our day-to-day activities. We are also indebted to the administration and staff of the HTWG Konstanz for their help, especially president Dr. Carsten Manz and Prof. Dr. Oliver Haase, for their support and for continuing the start-up funding, and the faculties of Mechanical Engineering, Electrical and Information Engineering, and Computer Science with the deans Prof. Dr.-Ing. Klaus Schreiner, Prof. Dr. Thomas Birkhölzer and Prof. Dr. Jürgen Neuschwander for their assistance. Furthermore we appreciate the support of the Institute for Applied Research (IAF) Konstanz, especially Prof. Dr.-Ing Horst Werkle and Dipl.-Ing. FH Andreas Burger.

Contents

Institute Profile	6
IOS Building and Location Plan	7
Institute Members	8
IOS Staff	10
External Fundings and Grants	11
Cooperations with Research Institutions and Industry	11
Theses and Student Projects	12
Publications	13
Research Activities	16
Deep Learning methods in Convolutional Neural Networks	17
Comparison of Deep Learning features with transformation codes	19
Reconstruction of Petershausen's Abbey Portal	21
Detection of flowmarks on laminated decor using texture features	23
Modeling of Decisions in Reef Fish with Machine Learning	24
Framelet-based image inpainting	26
LabellImage Tools	28
Automatic detection of context information in images with machine learning	30
Multi-resolution 3D Mesh Processing	32
3D Primitive Classification Using Stacked Autoencoders	34
A Virtual-Reality 3d-Laser-Scan Simulation	38
Morphed 3d fish models using multi-perspective 2d fish images	40
On-line splat rendering	44
Energieeffiziente Beleuchtung von Solitärobjekten	46
Melanopische Lichtwirkung - Aktuelle Erkenntnisse aus Forschung und Lichtplanung	48

Institute Profile

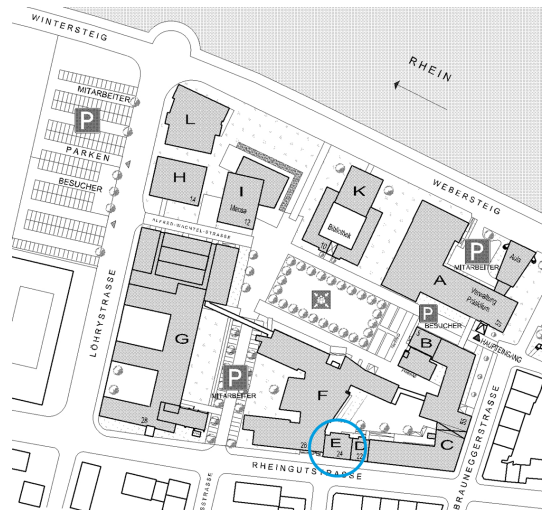


IOS BUILDING AND LOCATION PLAN



Institute for Optical Systems

Brauneggerstraße 55
Building E
3rd and 4th floor
78462 Konstanz



Location Plan

INSTITUTE MEMBERS

Prof. Dr. Georg Umlauf:



Diploma in computer science from University of Karlsruhe, 1996. Doctoral degree in computer science from University of Karlsruhe, 1999. PostDoc at University of Karlsruhe and University of Florida, Gainesville, USA, 1999-2000. Software development and senior researcher at Tebis AG, Hamburg, 2000-2002. Assistant professor for geometric algorithms at University of Kaiserslautern, 2002-2009. Interim professor for computer graphics at University of Karlsruhe, 2009. Since 2009 professor for computer graphics at University of Applied Sciences Konstanz and head of the computer graphics lab. Since 2010 member of the 'Institute for Optical Systems (IOS)' and 'Institute for Applied Research (IAF)'. Main research interests: Computer graphics, geometric modeling (splines, subdivision), reverse engineering, physical simulations.

Prof. Dr. Matthias Franz:



M.Sc. in Atmospheric Sciences from SUNY at Stony Brook, Diploma in physics from the Eberhard-Karls-Universität, Tübingen and doctoral degree in 1998. Thesis research in visual insect and robot navigation at the MPI for Biological Cybernetics and as a PostDoc at the Australian National University in Canberra. In industry he worked on various aspects of autonomous vision systems. 2002, he returned to the MPI as a group leader in the area of machine learning and computer vision. Since 2007 professor at the University of Applied Sciences in Konstanz and head of cognitive systems lab. Member of 'Institut für Angewandte Forschung (IAF)'. Main research activities in the development of automatically generated vision systems, optimisation and probabilistic modeling, with applications in industrial machine vision, texture analysis and steganalysis.

Prof. Dr. Claus Braxmaier:



Diploma in precision engineering at University of Applied Sciences Furtwangen. Diploma in physics and doctoral degree at the University of Konstanz in the field of fundamental tests of physics. Post-Doc at University of Konstanz. At EADS Astrium GmbH, system responsible for scientific and Earth observation missions for ESA and head of group 'Mission Metrology'. 2005-2013 professor for physics and control theory at the University of Applied Sciences Konstanz. Since 2013 ZARM Deputy Executive Director, Director Space Technology, and department lead "System Enabling Technologies" at the DLR-Institute of Space Systems, Bremen. Main research: high resolution optical metrology for industrial and space applications, tests of fundamental physics.

Prof. Dr. Bernd Jödicke:



Study of physics at the University of Karlsruhe. Doctoral degree at Technical University Hamburg and University Karlsruhe in the field of high frequency technology. After that, industrial work at ABB Baden, Switzerland, as executive director for R&D. Since 1992 professor for applied physics at University of Applied Sciences Konstanz. Member of 'Institute for Applied Research (IAF)', 'Institut für Naturwissenschaften und Mathematik (INM)', 'Institute for Optical Systems (IOS) Konstanz' and 'Deutsche Lichttechnische Gesellschaft'. Head of laboratory for light engineering at HTWG. Main research activities in color and light measurements and color camera systems.

Prof. Dr. Burkhard Lehner:



Diploma in computer science from University of Kaiserslautern, 2004. Doctoral degree in computer science from University of Kaiserslautern, 2008. Software development at Sirona Dental System GmbH, Bensheim, 2008-2013. Since 2013 professor for computer science at University of Applied Sciences Konstanz. Since 2014 member of the 'Institute for Optical Systems (IOS)'. Main interests: software development, computational geometry, optical 3D measurement (especially in dental CAD/CAM).

Prof. Dr. Klaus-Dieter Durst:



Study of physics at the University of Stuttgart, 1986 doctoral degree in the field of magnetism at the Max-Planck-Institute of metal research. Thereafter research center Weissach of the Dr. Ing. h.c. F. Porsche AG, responsible for the central unit 'measurement technologies'. Since 1993 professor for measurement engineering and sensor technology at the University of Applied Sciences Konstanz. Member of 'Institut für Naturwissenschaften und Mathematik' and 'Institute for Optical Systems' Konstanz. Head of laboratories for measurement and sensor technology and production metrology. Currently director of 'Institut für Naturwissenschaften und Mathematik' Konstanz. Activities in the accreditation and surveillance of testing laboratories and inspection bodies.

Prof. Dr. Christian Hettich:



Diploma in physics and doctoral degree (2002) at the University of Konstanz in the fields of quantum-optics and nano-optics. Post-doc at the Eidgenössische Technische Hochschule (ETH) Zürich and at the Niels Bohr Institut in Kopenhagen. Systems engineer for illuminators of semiconductor lithography systems at Carl Zeiss SMT GmbH in Oberkochen. Systems engineer for time-of-flight cameras at ifm automotive GmbH in Kressbronn. Project leader for automated microscopes at Sensovation AG in Radolfzell. Since 2014 professor for physics, feedback control systems and metrology at the department of mechanical engineering of the University of Applied Sciences Konstanz. Member of the 'Institut für Naturwissenschaften und Mathematik' (INM) and the 'Institute for Optical Systems' (IOS). Main research interests: optical 3D measurements, spectroscopy, interferometry, holography, microscopy.

IOS STAFF

Professors

Georg Umlauf, director IOS
Matthias Franz, associate director IOS
Claus Braxmaier
Bernd Jödicke
Burkhard Lehner
Klaus-Dieter Durst
Christian Hettich

Officer

Pascal Laube

Academic Staff

Leonard Thießen
Martin Miller
Mirco Indlekofer
Theresa Kocher
Dennis Grießer
Fabian Freiberg
Tobias Birkle
Marco Fehrenbach

Postdoc

Thilo Schuldt

PhD Students

Michael Grunwald
Martin Schall
Pascal Laube
Jürgen Keppler

EXTERNAL FUNDINGS AND GRANTS

- Baumer Inspection GmbH, Konstanz: "Farbtexturen in der industriellen Oberflächeninspektion", contract research.
- Baumer Inspection GmbH, Konstanz: "Inline - Inspektionstechnologie zum Farbabgleich für den digitalen Dekordruck", contract research.
- Australian Research Council, Pattern recognition in animals and machines: using machine learning to reveal cues central to the identification of individuals, Discovery Projects Grant.
- BMBF-Grant "Forschung für die Produktion von morgen" 2015, Entwicklung einer innovativen Anlagentechnik zur automatisierten und laserbasierten Reparatur strukturierter Formeinsätze - ToolRep.

COOPERATIONS WITH RESEARCH INSTITUTIONS AND INDUSTRY

Academic and Institutional Cooperations

- University of Queensland, Brisbane
- Humboldt-Universität zu Berlin
- ZARM (drop tower), Center of Applied Space Technology and Microgravity, Bremen
- DLR Institut für Raumfahrtssysteme Bremen
- University of Tübingen
- Max-Planck-Institute for Biological Cybernetics, Tübingen
- German Federal Office for Information Security (BSI), Bonn
- Universität Konstanz
- University of California, Davis
- Technische Universität Kaiserslautern
- University of Florida, Gainesville
- Grenoble Institute of Technology
- University of Strasbourg

Industry Cooperations

- Siemens Postal, Parcel & Airport Logistics GmbH, Konstanz
- Sirona GmbH, Bensheim
- EADS Astrium, Immenstaad
- Breuckmann GmbH, Meersburg
- Chromasens GmbH, Konstanz

- Baumer Inspection GmbH, Konstanz
- Procon-System GmbH, Thierstein
- Lightdesign-Solutions GmbH, Dresden
- Knotenpunkt, Wenzel Präzision GmbH, Balingen
- Tebis AG
- Liebherr Aerospace GmbH, Lindenberg
- NTT Data Deutschland GmbH
- Lacuna Solutions GmbH
- EUTECH GmbH
- Siegfried Hofmann GmbH
- ACSYS Lasertechnik GmbH
- Fraunhofer Institute for Production Technology IPT

THESES AND STUDENT PROJECTS

PhD Theses

- Bartolomiej Piotr Siwek, Discrete methods for splines and subdivision curves, University of Oslo, 2015.

Master Theses

- Matthias Hermann, Methoden des Deep Learning im Bereich Convolutional Neural Networks, 2015.
- Merlin Blume, 3D Primitive Classification Using Stacked Autoencoders, 2015.
- Patrick Mutter, Automatische Bestimmung von Kontextinformationen aus Bildern mit maschinellem Lernen, 2016.
- Manuel Hieke, Texture recognition based on texton analysis and machine learning algorithms, 2016.
- Martin Miller, Adaptive B-Spline Activation Function for Neural Networks, 2016.
- Mirko Indlekofer, Merkmalsbasierte Objekterkennung mit Methoden des maschinellen Lernens, 2016.
- Theresa Kocher, Defect Detection Using a Parametric Texture Model, 2016.
- Timo Hamm, Vergleich künstlicher neuronaler Netze mit Transformations-Codes, 2016.
- Marco Fehrenbach, Physikalische Simulation für einfache Kamerasysteme, 2016.

Bachelor Theses

- Felix Peter, Optische Selbstlokalisierung eines 3D-Druckkopfes im dreidimensionalen Raum, 2015.
- Tarek Schneider, VR-Scan-Simulation Raycasting von Spline-Flächen, 2015.
- Malvin Danhof, VR-Scan-Simulation Raycasting von Dreiecksnetzen, 2015.
- Tobias Offerdinger, Simulation und Auswertung optischer Filter mit Hilfe eines multispektralen Aufnahmesystems, 2015.
- Benjamin Kugler, Simulation von Objekteigenschaften anhand radiometrischer Referenzdaten, 2015.
- Robin Mattes, Optische Detektion von Düsenfehlern im Inkjet-Druck, 2015.
- Tobias Birkle, Simulation von Kamerasensoren anhand radiometrischer Referenzdaten, 2015.
- Jens Gansloser, Radiometric calibration of digital cameras using sparse Gaussian processes, 2016.
- Tung Pham, Framelet-Based Image Inpainting, 2016.
- Julian Schneider, Multiskalen Signalverarbeitung von Dreiecksnetzen, 2016.
- Fabian Freiberg, Implementierung eines Convolutional Neural Networks mit CUDA, 2016.
- Dennis Griebner, Geometrische Kalibrierung von Stereokameras, 2016.

Student Projects

- David Simon, Dennis Bleicher, Jürgen Rieg, Point Cloud Label Tool, 2015.
- Simon Kesser, Tobias Keh, Felix Born, Surface Subdivision Tool, 2015.
- Janine Panske, Christian Hümmer, 3d-Rekonstruktion romanisches Portal, 2016.
- Felix Hinderer, Patrick Fiur, Robert Kleinhaus, 3d-Fischrekonstruktion, 2016.

Journal Papers

- Schuldt, T., C. Schubert, M. Krutzik, L. Bote, N. Gaaloul, J. Hartwig, H. Ahlers, W. Herr, K. Posso-Trujillo, J. Rudolph, et al., "Design of a dual species atom interferometer for space", *Experimental Astronomy*, vol. 39, no. 2, pp. 167-206, 2015.

Conference Proceedings

- Denker, K., B. Hamann, and G. Umlauf, "On-line CAD Reconstruction with Accumulated Means of Local Geometric Properties", *Curves and Surfaces, 8th International Conference, Paris 2014*: Springer, pp. 181-201, 2015.
- Grunwald, M., J. Müller, M. Schall, P. Laube, G. Umlauf, and M. O. Franz, "Pixel-wise Hybrid Image Registration on Wood Decors", *BW-CAR— SINCOM*, pp. 24, 2015.
- Schall, M., M. Grunwald, G. Umlauf, and M. O. Franz, "Radiometric calibration of digital cameras using Gaussian processes", *SPIE Optics+ Optoelectronics: International Society for Optics and Photonics*, 2015.
- Danhof, M., T. Schneider, P. Laube, and G. Umlauf, "A Virtual-Reality 3d-Laser-Scan Simulation", *BW-CAR— SINCOM*, pp. 68, 2015.
- Schall, M., M-P. Schambach, and M. O. Franz, "Improving gradient-based LSTM training for offline handwriting recognition by careful selection of the optimization method", *Conference: BW-CAR Symposium on Information and Communication Systems (SInCom)*, 12/2016.
- Schall, M., M-P. Schambach, and M. O. Franz, "Increasing robustness of handwriting recognition using character n-gram decoding on large lexica", *12th IAPR International Workshop on Document Analysis Systems: IEEE*, 2016.
- Grunwald, M., J. Gansloser, and M. O. Franz, "Radiometric calibration of digital cameras using sparse Gaussian processes", *Workshop Farbbildverarbeitung*, 2016.
- Laube, P., and G. Umlauf, "A short survey on recent methods for cage computation", *BW-CAR— SINCOM*, pp. 37, 2016.
- Grunwald, M., and M. O. Franz, "Wahrnehmungsorientierte optische Inspektion von texturierten Oberflächen", *INFORMATIK 2016, Lecture Notes in Informatics (LNI) Gesellschaft für Informatik*, vol. 259, pp. 1963-1968, 2016.

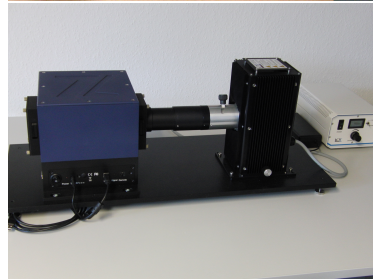
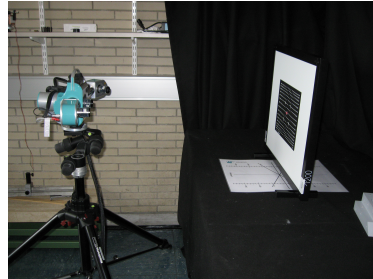
Laboratories and Infrastructure

The Institute for Optical Systems laboratories and infrastructure is composed of scientific equipment from the fields of Image Sensing, 2D and 3D Surface Analysis and Reconstruction as well as a powerful computing cluster for machine learning and high performance computing. Our laboratories and infrastructure is located in buildings *E*, *G* and *O* on the university campus.

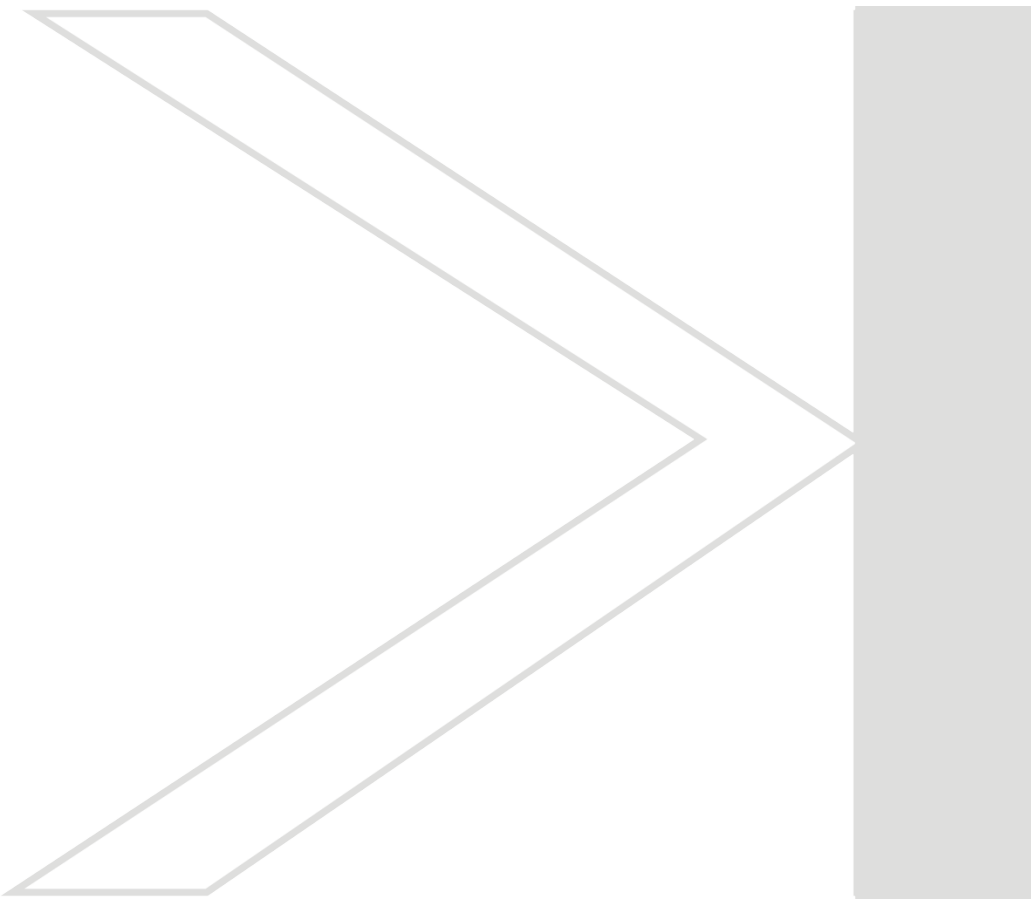
The laboratory in building *G* includes equipment with focus on illumination engineering and high precision stereoscopic surface scanning. The laboratory in building *E* comprises of camera calibration and spectrometric color measurement equipment, multispectral cameras as well as devices for 3D laserscanning, 3D visualization and 3D printing.

The computing cluster located in building *O* consists of GPU as well as CPU-Servers for high performance computing.

Most of the institutes workspaces are located on floors three and four of building *E*.



Research Activities _____



Deep Learning methods in Convolutional Neural Networks

Matthias Hermann, Martin Schall and Matthias O. Franz

Research in Artificial Neural Networks has seen important improvements in shape of Deep Learning [?] and Deep Neural Networks in recent years. This effort lead for example to the first computer system capable of beating human masters in the game of Go [?]. We conducted broad research into the field of Deep Learning, especially Convolutional Neural Networks [?] to implement these methods and reproduce the reported results. This work provides a foundation for further research with Artificial Neural Networks and applying these to real-world problems at the Institute for Optical Systems.

Introduction

Artificial Neural Networks started out as mathematical models of biological neurons and neural networks in the 1950's. Since then they have been subject of many studies and research and have been developed into a machine learning method suitable for a wide range of tasks like classification, regression, object detection, feature extraction or handwriting recognition. They consist of networks of artificial neurons, each providing only very basic mathematical function, but the combined network is capable of approximating highly non-linear functions [?]. Training of Artificial Neural Networks is done by applying a large data set with known in- and outputs, 'showing' one sample at a time to the network and correcting the error done at each sample. This so called supervised training using the backpropagation algorithm was first successfully applied to Deep Neural Networks in 2006 [?] and has since allowed a wide variety of research and applications in Deep Learning.

Convolution Neural Networks [?] are well suited for tasks with image (e.g. objects or textures) or geometric (e.g. point clouds) input. They allow the automatic end-to-end learning of low-level filters like edge detectors combined with high-level tasks like object classification. This makes them a research interest for a number of projects at the Institute for Optical Systems.

The presented work consists of a structured inquiry of state-of-the-art methods in Convolutional Neural Networks, as well as the implementation and evaluation of these methods. The work reproduced published results on public databases with the same or near same quality as documented in the publications.

Methods and findings

An implementation of Convolutional Neural Networks and related training algorithms has been done on basis of state-of-the-art publications in the field. It has been successfully applied to the MNIST handwritten digit database and CIFAR10 object database. CIFAR10 consists of images of ten different classes (e.g. dogs or airplanes) with the task of correctly classifying the image. Figure 1 shows the first layer of convolutional kernels of a network trained for this task. It shows an interesting observation with Convolutional Neural Networks: The first convolutional layer learns Gabor-like filter kernels that are also present in the early vision in nature. This is an example of Artificial Neural Networks imitating biological functionality without explicitly training the network to achieve this.

The end-to-end classification with a CNN is then performed by repeatedly applying convolutional kernels and feature extraction to the data. This allows to extract a few high-level features (the classification of each sample) from many low-level features (the image's pixels colors).

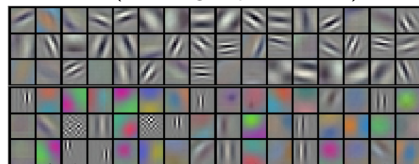


Figure 1: Convolutional kernels for object classification. Image by Alex Krizhevsky [?]

The presented work also includes the evaluation of improvements for Convolutional Neural Networks and their training methods:

- Optimization methods, e.g. Stochastic Gradient Descent, Nesterov Momentum, RMSProp, AdaDelta, Equilibrium SGD.

- Regularization methods: L1-, L2-regularization, early stopping and dropout learning.
- Max, average and stochastic pooling layers.
- Visualizations of Convolutional Neural Networks and their training process.

Classification-, regression- and autoencoder-tasks were tackled in the presented work. Figure 2 shows the convergence of training and validation error rates for MNIST - the task of classifying handwritten digits zero to nine - with different optimization methods. The topology, hyper-parameters and initialization of the network itself was kept constant over all experiments. It shows that choosing a suitable optimization method is critical for speeding up the convergence rate and overall error rate. This is an observation that can be made for other aspects in Deep Learning as well: Good results can be achieved quickly with basic approaches, but correctly handling the details lead to the best results in the end.

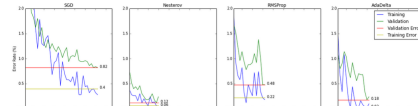


Figure 2: Convergence of training and validation error rates for MNIST

Next steps

The presented work successfully implemented and evaluated state-of-the-art methods of Convolutional Neural Networks at the Institute for Optical Systems. This allows further research into this topic and the application of the gained knowledge to running and future projects. Of particular interest are applications in object detection, texture analysis and geometric reconstruction. Other successfully applications like playing the game of Go [?] at a master's level or recognizing the geolocation of vacation pictures [?] show that Convolutional Neural Networks can be applied to a wide variety of problems. This reinforces the research and application of a Deep Learning approach to more visual and geometric problems.

Comparison of Deep Learning features with transformation codes

Timo Hamm, Martin Schall and Matthias O. Franz

Research in Artificial Neural Networks has seen important improvements in shape of Deep Learning [?] and Deep Neural Networks in recent years. An important research field in Deep Learning are Convolutional Neural Networks [?], which have proven to be effective for image classification and segmentation [?] and general spatially correlated [?] problems. Convolutional Neural Networks are often organized in a great amount of layers [?] with feature extraction layers in the front. This work includes a series of experiments to determine if feature extraction of Convolutional Neural Networks can be improved or simplified by applying transformation codes, e.g. Principal Component Analysis or Independent Component Analysis, to the raw input data.

Introduction

Convolutional Neural Networks (CNN) are a type of artificial neural networks that use repeated folding and subsampling to reduce the spatial resolution of inputs and extract meaningful features. CNNs thus require data with spatial correlation, but are indeed very successful in handling these type of data. Typical applications of CNNs include image classification [?], often organized in very deep networks [?]. The first layers of a CNN are known [?] to extract simple geometric features from input images. On the other hand are deep networks inherently more difficult to train [?] than shallow networks. It is thus in the interest of the scientist or practitioner to reduce the number of layers of a artificial neural network if possible.

The presented work showcases our experimental study at the Institute for Optical Systems that aims at reducing the number of layers of a CNN by application of transformation codes like Principal Component Analysis (PCA) or Independent Component Analysis (ICA) on the raw input. PCA or ICA could even be included into a neural network by initializing the first layers of a CNN to the extract the features detected by the PCA or ICA component analysis.

Methods and findings

Experiments in this work were started by training CNNs for the publicly available MNIST and CIFAR10 data sets. MNIST contains 60k black-and-white images of size 28x28 of handwritten digits zero to nine. CIFAR10 contains 60k RGB-images of size 32x32 belonging to ten different classes, like e.g. dogs or cars. State-of-the-art network topolo-

gies and optimization methods were used for both CNNs.

Next step was the comparison of the features extracted by the first convolutional layer with the components extracted by PCA or ICA. To accomplish this, square patches of equal size were extracted from the images. The size of the square patches were identical to the convolution size of the first CNN layer. Patches were analysed using PCA and ICA and their component being transformed back into the image space. This allows to visually inspect the extracted features or components, as shown in Figures 3, 4 and 5.

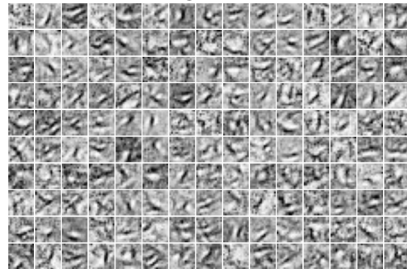


Figure 3: Features extracted by the first convolutional layer of a CNN. Patches are of size 15x15 from the MNIST data.

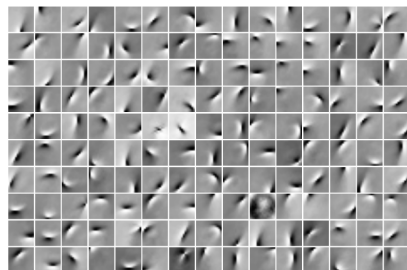


Figure 4: Components extracted by ICA. Patches are of size 15x15 from the MNIST data.

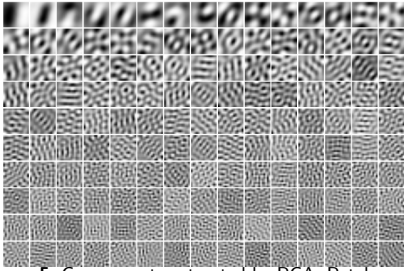


Figure 5: Components extracted by PCA. Patches are of size 15x15 from the MNIST data.

Several statistical comparisons of the features extracted by CNN and the components of PCA and ICA were conducted. These included the comparison of the feature orientation and its bandwidth, as well as feature spatial frequency and its bandwidth. A modified variant of χ^2 was used to compare these attributes of the extracted features.

The statistical comparison revealed a strong

correlation of ICA and CNN features in spatial frequency, but also of PCA and CNN features in orientation. Correlations between ICA, PCA and CNN in orientation were in similar ranges and thus a generally higher correlation between ICA and CNN features than PCA features was shown.

Next steps

The presented work successfully showed a correlation between PCA and ICA components as compared to CNN features. This allows further research into the topic, e.g. by initialization of coefficients within a CNN to resemble the components extracted by PCA or ICA. This could lead to speed-ups in training time of CNNs or the reduction of necessary layers within a CNN. Other possible applications include the implementation of curriculum learning [?] by using clustering methods on basis of extracted PCA or ICA components.

Reconstruction of Petershausen's Abbey Portal

Christian Hümmer, Janine Panske, and Georg Umlauf

This project is concerned with the 3d reconstruction of the roman portal of the former minster of Petershausen. The only remains of this portal consist of the tympanum, the brow-piece, four capitals and two jamb statues. These artifacts are exhibited at the Badische Landesmuseum, Karlsruhe.

The goal is to digitize these artifacts as good as possible to allow for a subsequent 3d reconstruction. To this aim various scanning technologies were used. Each device yields different types of data at different resolutions and different noise signatures. However, finally only one merged, de-noised, and compressed 3d model of the artifacts is required.

Introduction

The abbey in Petershausen was founded in the 10th century. The minster was teared down 1831 and the remains of the portal were shipped to Eberstein. The respective artifacts of the portal of the minster were made between 1173 and 1180, see Figure 6 (left). The two jamb statues portray pope St. Gregor I. (590 – 604) and St. Gebhard II., bishop of Konstanz and founder of the abbey (979 – 995) They are made of yellow-gray colored sandstone, which was exposed to various environmental stresses like weather-caused erosion, a fire, and multiple dismounting, transportation, and re-mounting procedures. Thus, the remains are broken, disconnected, and details are eroded. The height of the complete portal is up to four meters and weights several tons.

These remains are in a permanent exhibition in the Badischen Landesmuseum in Karlsruhe, see Figure 6 (left). However, this permanent exhibition is timbered in a closed and tight wooden shed. This means, that the accessibility is very limited and the lighting situation is extremely difficult, see Figure 7.



Figure 6: Con-temporal painting of the minster's portal of Petershausen (left) and current display in the Badischen Landesmuseum, Karsruhe, (right) [1]. Courtesy: Badisches Landesmuseum.



Figure 7: During the scanning.

Project description

In October 2016 a team of several students and staff from HTWG as well as from our industry partner FARO meet in Karlsruhe for the digitization of the artifacts. For the digitization of the artifacts various scanning techniques and devices have been used:

- FARO laser-line probe, a manual laser scanner mounted on a measuring arm. Reconstruction results are shown in Figure 8.
- FARO Freestyle 3D, a manual structured-light scanner. Reconstruction results are shown in Figure 9.
- Structure Sensor, a manual infrared structured-light scanner. This techniques yield results that could not be used for a detailed reconstruction.
- Photogrammetry based on digital camera images and a subsequent Agisoft-

reconstruction. Reconstruction results are shown in Figure 10.

The complete reconstruction process consists of four stages

1. digitization,
2. point cloud processing (registration, sub-sampling, de-noising, etc.),
3. mesh generation (Poisson, ball-pivoting, etc.), and
4. post processing (texturing, etc.).

The final 3d models of the artifacts were provided to the Faculty of Architecture of HTWG, to be used in the design of a complete physical reconstruction of the portal at its original location, and to a toy manufacturer to reproduce the two jamb statues at a size of ca. 30 cm for the Verein Petershauser Orgelkultur as artwork presents [2].



Figure 8: Laser-scanner reconstruction of the jamb statue of pope Gregor I.



Figure 9: Structured-light scanner reconstruction of the tympanum and the brow-piece.



Figure 10: Photogrammetric reconstruction of the portal.

Bibliography

- [1] https://www.leo-bw.de/en_US/web/guest/detail-gis/-/Detail/details/DOKUMENT/blm_museumsobjekte/8A4B2C47F3AF49488B6F0F6BE6EF871D/Kirchenportal+Kirchenportal+sog+%22Petershausener+Portal%22
- [2] <https://www.petershauser-portal.de/>

Detection of flowmarks on laminated decor using texture features

M. O. Franz, H.-P. Diehl¹

The production process of laminated decors is subject to a large variety of perturbations some of which are very hard to detect by machine vision algorithms. Among the most notorious are flowmarks that are caused by processing errors during lamination. Flowmarks are only visible in certain lighting and viewing conditions, and only show up with a very small texture contrast. In this project, we developed a new detection algorithm for flowmarks that is based on higher-order texture features in combination with support vector classifiers.

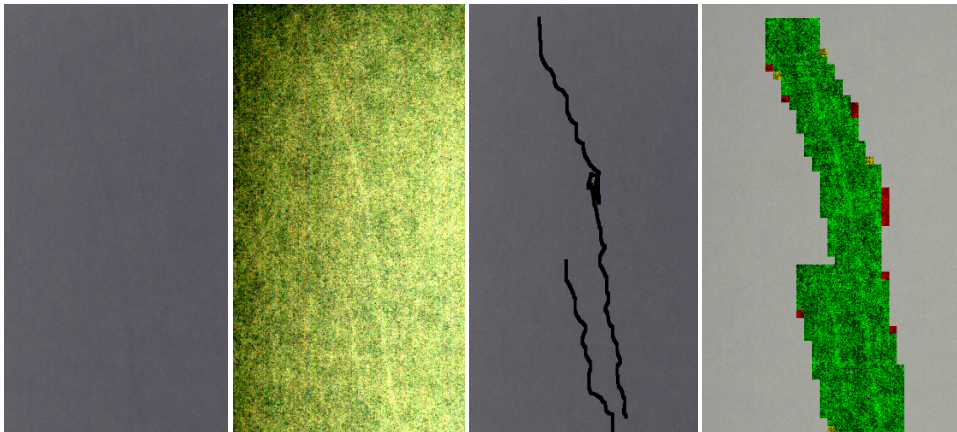


Figure 11: *Left:* Example of flowmarks on a laminated decor shown in the original contrast; *middle left:* Contrast maximized image of the flowmarks; *middle right:* Hand labeling for training and testing the detection system; *right:* detector output - detected regions that contain flowmarks are marked in green, erroneous detections in red.

Flowmarks usually appear as low-contrast linear structures that are very hard to detect in a textured background (see Fig. 1, left). However, to the human eye these structures are still visible under certain viewing angles and possibly disturbing. From the point of view of machine vision, flowmarks are particularly hard to detect as they show themselves only by small alignments of texture elements, not by different contrasts or colors. In terms of statistics, this means that flowmarks can only be detected by analyzing higher-order pixel dependencies, i.e. dependencies between three or more pixels. We therefore used higher-order tex-

ture features that were previously only applied to problems in steganalysis². For training our detector, we labelled flow marks by hand and subsequently divided the images in overlapping regions (see Fig. 1, middle right). The texture in each region was characterized by its higher-order features which comprised the input to a support vector machine. The training of the detector required about 5000 image regions before a satisfactory detection rate could be achieved. The trained detector has a very low false alarm rate while correctly marking the majority of all image regions contaminated by flowmarks (see Fig. 1, right).

¹Baumer Inspection GmbH, Lohnerhofstrasse 6 78467 Konstanz

²Pevny, T., et al.: Steganalysis by subtractive pixel adjacency matrix. IEEE Trans. Info. Forensics and Security, 5(2), 215-224, 2010.

Modeling of Decisions in Reef Fish with Machine Learning

M. O. Franz, U. Siebeck*, A. Parker*, G. Wallis*

*School of Biomedical Sciences and School of Human Movement and Nutrition Sciences, The University of Queensland

Some reef fish are capable of visually recognizing thousands of different individuals although they do not dispose of any evolutionary advanced cortical structures in their brains. Often tiny differences in the facial patterns are the only visual cues available for this task, but it is still unknown which of these cues might play a role in the recognition process. In our study, we use machine learning models of the underlying decisions to identify these cues and to assess their relative importance.

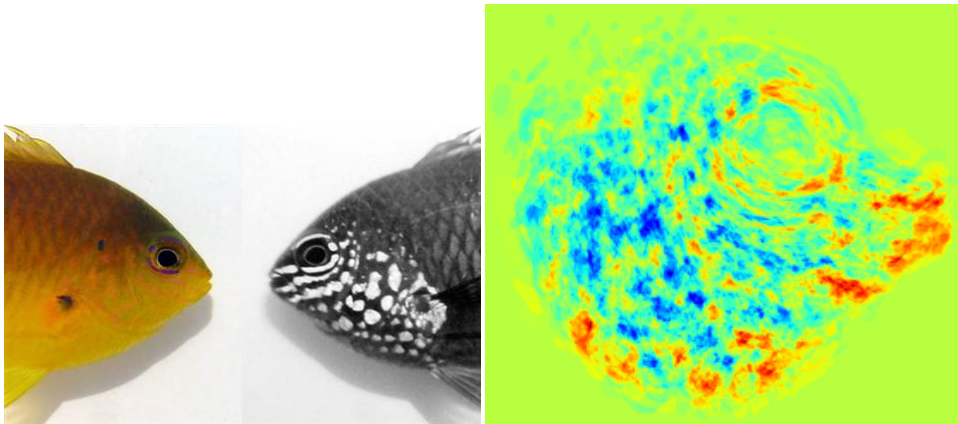


Figure 12: Left: Damselfish (appearance in the visual range is shown left) can distinguish between conspecifics by looking at the ultraviolet patterns on their faces (appearance in the UV range is shown right). Right: A color coded map of the relevance of each facial region for recognizing this fish species (decision image) obtained from machine learning. Green regions are irrelevant, red regions have a positive weight for the decision, blue regions a negative weight.

Superficially, fish might not appear to be the first choice for being studied by a neurobiologist as they do not possess any evolutionary advanced brain structures such as the cortex in the mammalian brain. But exactly this makes them interesting from a neurobiological point of view: although their brain structure might be comparatively simple, fish (and particularly reef fish) sometimes show astonishing cognitive capabilities. Cleaner fish, for instance, often discriminate between thousands of "customer" fish and adapt their cleaning behaviour to the individual needs and preferences of the customer. In humans and mammals, such behavior usually involves cortical brain structures, but fish achieve this by using

a much more primitive neural architecture. This simplicity opens up the opportunity for neurobiology to understand higher cognitive functions by studying simple neural architectures.

The present project is a collaboration between neurobiologists of the University of Queensland, Australia, and the IOS Konstanz. We focus on the visual discrimination between certain species of reef fish which is based on complex facial patterns (visible in the ultraviolet range, see Fig. 1). The exact nature of the visual cues used for this task was still unknown at the onset of the project, so the goal was to identify these cues and assess their relative importance.



Figure 13: Laboratory environment for conducting fish experiments. The fish are captured in the wild and kept in individual tanks. They are trained to discriminate between various fish species by presenting them images and rewarding a correct choice.

To achieve this goal, we conducted a large number of behavioral experiments with captured reef fish in the laboratory of Dr. Siebeck. In each experimental trial, the fish was presented facial images from two different fish species (a target and a distractor species, see Figs. 2,3). When the fish swam to the target fish species it was supposed to learn, it received a reward. After training, the recognition performance of the fish was tested on new, previously unseen images to make sure it actually learnt the discrimination task. At the same time, we trained a learning machine on exactly the same image data to reproduce the behavioral decisions of the fish as closely as possible. In this way, the learning machine became a mathematical model of the underlying decision process of

the fish.

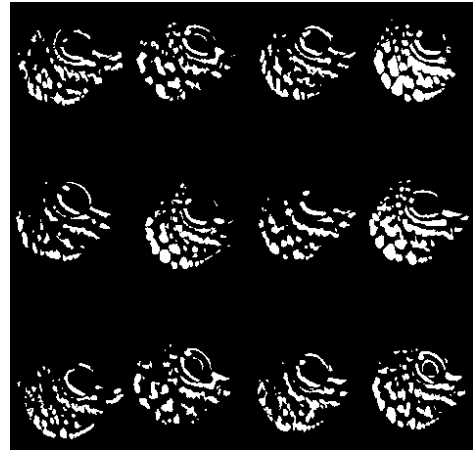


Figure 14: Binarized facial patterns used for training the fish and the learning machine in the experiments.

In contrast to the fish brain, the trained learning machine can be directly analyzed. We extracted so-called *decision images* which may be interpreted as a map that associates a weight to each image region (Fig. 1). The weight indicates the relevance of the image region for the decision process. Image regions which are important for discriminating the target fish species have a high positive weight, image regions which are important for recognizing the distractor species a high negative weight. The example in Fig. 1 shows that the modelled fish used the eye region and the lower part of the facial pattern for recognizing the target species.

Framelet-based image inpainting

Tung Pham, Pascal Laube and Georg Umlauf

Image inpainting is an important problem in the domain of image processing. Tight wavelet frames which are a specialization of well knot wavelets have recently been successfully applied to the problem of image inpainting [1]. In this project we evaluated the performance of framelet-based image inpainting on classic test images.

Introduction

Filling missing regions in images is a prominent topic of image processing. Image inpainting may help in image transmission, image coding or restoration. Many popular methods use the principle of filling a missing region by sampling from a "healthy" surrounding region. Results should look reasonable to a human observer. In this project we use wavelet tight frames or framelets for image inpainting. By first transforming the image to the framelet domain and applying thresholding in this domain one can fill in previously unknown information.

Method

Let $\langle \cdot, \cdot \rangle$ and $\| \cdot \|^2$ be the dot product and norm of $L_2(\mathbb{R})$. A wavelet-system $X(\Psi)$ is a family of scaled and translated wavelets of finite set $\Psi \subset L_2$:

$$X(\Psi) = \{ \psi_{s,u} : \psi \in \Psi, \quad s, u \in \mathbb{Z} \}$$

Elements ψ of Ψ are called generators. A system $X(\Psi)$ is called *Bessel-system*, if there exists an upper bound

$$\sum_{g \in X(\Psi)} |\langle f, g \rangle|^2 \leq B \| f \|^2, \forall f \in L_2(\mathbb{R}), B > 0.$$

A Bessel-system $X(\Psi)$ is called *frame*, if there exists a lower bound

$$\sum_{g \in X(\Psi)} |\langle f, g \rangle|^2 \geq A \| f \|^2, \forall f \in L_2(\mathbb{R}), A > 0.$$

If $A = B$ this is called a *tight frame*:

$$\sum_{g \in X(\Psi)} |\langle f, g \rangle|^2 = \| f \|^2, \forall f \in L_2(\mathbb{R}), A = B = 1.$$

If $X(\Psi)$ is a tight frame, generators $\psi \in \Psi$ are called *tight framelets*. Compared to orthonormal wavelets, tight framelets are redundant. This redundancy can be exploited for the purpose of inpainting.

The inpainting process consists of four steps:

1. By applying an analysis operator the image is first transformed to the framelet domain where it is represented by its framelet coefficients.
2. To propagate information into the defective region framelet coefficients are thresholded.
3. By then synthesizing back to the image domain with thresholded coefficients missing information is filled.
4. For smooth transition this process is repeated until converge criteria are met.

Hard thresholding is defined as

$$T(c_n) = \begin{cases} 0, & |c_n| \leq T, \\ c_n, & \text{sonst} \end{cases}$$

with framelet coefficients c_n and threshold T . By applying this hard threshold small coefficients are completely removed. This also suppresses static noise. An open question is the selection of T . Large T results in missing detail while small T leads to insignificant changes.

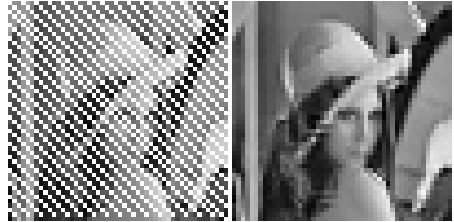
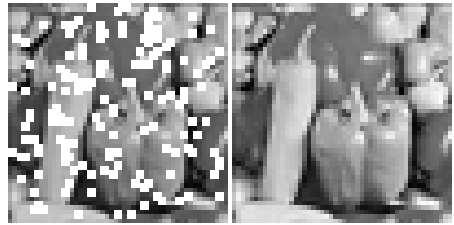
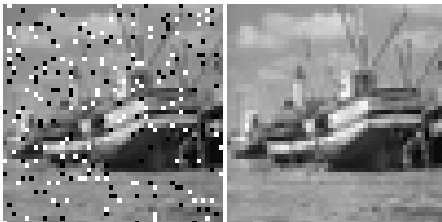
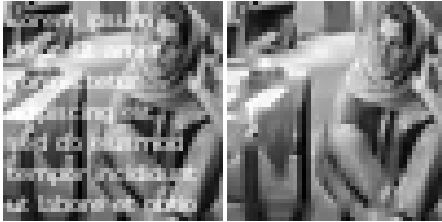
For *soft thresholding* every coefficient receives an individual threshold value.

$$t_{\lambda_i}(c_n) = \begin{cases} 0, & |c_n| \leq \lambda_i, \\ \text{sgn}(c_n)(|c_n| - \lambda_i), & |c_n| > \lambda_i \end{cases}$$

While low-pass coefficients are not manipulated in hard-thresholding they are in soft thresholding. This can help the inpainting process.

Results

Following we show some results of framelet-based inpainting.



Bibliography

- [1] Cai, Jian-Feng and Chan, Raymond H and Shen, Zuowei: A framelet-based image inpainting algorithm. *Applied and Computational Harmonic Analysis*, 24, 131–149, 2008.

LabelImage Tools

Sonja Futterknecht, Tobias Birkle, Benjamin Kugler, Robin Mattes and Michael Grunwald

Machine learning needs a lot of training data to detect objects in images. To generate the training data, we developed a software solution to label and classify fishes in images. This project was in cooperation with the Global Change Institute of the University of Queensland.

Introduction

Regarding the number of fishes and their diversity it is possible to investigate the consequences of the climate change in coral reefs. This is the project of the Global Change Institute (GCI) at the University of Queensland under the head of Prof. Dr. Ove Hoegh-Guldberg. In order to specify the number of fishes experts dive through the coral reefs and document the fish population. Another project at the GCI is the *XL Catlin Seaview Survey*, in which coral reefs are photographed using underwater cameras, as shown in figure 15. The images of the reefs are published on the website globalreefrecord.org. The *FishNet* project, under the management of Dr. Ulrike Siebeck from the GCI wants to use the underwater photos of the coral reefs from the *XL Catlin* project to identify fishes and their number in the images. To detect the fishes a software solution will be developed using methods of machine learning. In the first step the fishes have to be labeled and classified in the photos manually to extract their features. For this part of the software solution a software called *LabelImage* is developed to label and classify the fishes. These labeled fishes are the training images

for the machine learning. Based on the training images the features of the fishes will be learned and it will be able to find these features in not yet labeled images. The manual labeling and classification of the fishes will be done by the experts of the *FishNet* team.

Current Work

The software was developed with Python 3.4 and PyQt 5. With this application a rectangle can be drawn around the fishes with one mouse click to label and classify them (see fig. 16). The coordinates of the labeled area and the corresponding fish species will be saved in an XML document. In a separate extraction module of the software the labeled fishes will be extracted from the original image with the help of the XML document. The extracted patches will be saved as single images. The patches can be used as training images for the machine learning. They form the basis for the automatic identification of the fishes. The determination of the species diversity and the number of the fishes works the better the more data is available for the software solution. To submit many fishes and thus training data to the soft-



Figure 15: *XL Catlin Seaview Survey* expert diving through coral reef. (globalreefrecord.org)

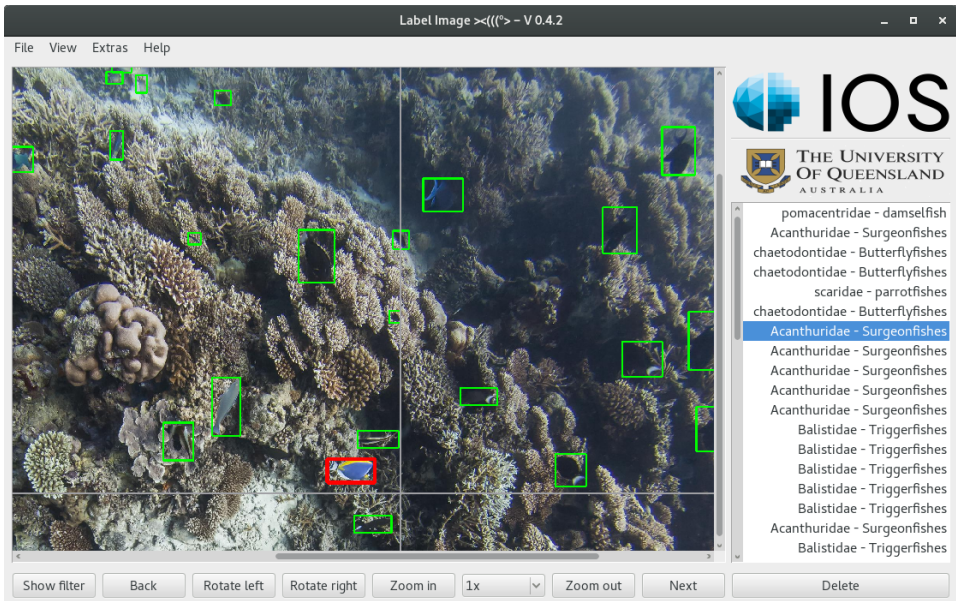


Figure 16: LabelImage software with labeled fishes.

ware solution the fishes are not only labeled by the scientists of the GCI but also by interested users. Therefore in the second part of the team project a web based software solution was developed using HTML5 and the JavaScript framework jQuery which allows the labeling and classification of the fishes. The software solution is embedded in an online course at the Massive Open Online Course platform *edx.org* and developed additionally as a standalone website. The labeled data will be saved in the same XML format as in the *LabelImage* software. Thus the extraction module of the software can be reused for the labeled patches in the web based software. The students will be evaluated by the number of labeled fishes, with an especially developed evaluation software of the team project. For the evaluation a reference image is used in which the fishes are already identified by the experts of the GCI. If the results are satisfying it can be assumed that the following images will be labeled equally well. These data contributes to the machine learning for the automatic identification of the fishes. The online course will be repeated every eight weeks to collect training images for the *FishNet* project. During the first two weeks after the activation of the course at the platform *edx.org* over 300 participants took part in the course. Thereby over 13500 fishes were found in 600 images. In comparison to that, the experts of the *FishNet* team labeled 5358 fishes in

four weeks. The experts first selected eleven fish species that the participants could then associate with the fishes in the pictures. In average the participants labeled 80% of the pictured fishes and associated 25% to a fish species.

Conclusion and Outlook

In summary it can be said that fishes can be labeled and classified in images with the *LabelImage* software solution by the scientists and with the web based software solution by other participants. With the evaluation software participants from the online course and the standalone website can be evaluated and the labeled fishes can be processed for the machine learning. Using these images the software can be trained and the classification of the fishes will be optimized. The software solution for identifying the fishes should facilitate the work of the scientists from the GCI. They do not have to classify the fishes manually anymore. With the underwater images from the *XL Catlin* project and the software solution the changes of the fish population in the coral reefs all over the world can be captured faster. The machine learning can be also used for detecting other objects in images, if there are enough training images available. Therefore any images can be loaded to the *LabelImage* software and then the desired objects can be labeled and classified.

Automatic detection of context information in images with machine learning

Patrick Mutter, Matthias O. Franz, Michael Grunwald

Machine learning provides several methods for image classification. We compare two methods of them to classify and detect content in images automatically. Two image datasets HIM-10.1 and HIR-10.1 are created. HIM-10.1 uses 60.000 images from existing public datasets, that matches the defined classes, while HIR-10.1 is built of 100.000 images under creative common license. As first approach support vector machines using histograms of oriented gradients as feature descriptors, are used to classify the images. Therefore, its need to find useful parameters to calculate hog-descriptors that describes all classes well. With convolutional neural networks a modern approach from deep learning is used to classify the image data. Using Nesterov-Momentum other hyper parameter and convenient model are searched to reach a good detection ratio. Finally we show that using CNNs with the datasets need less preprocessing and reach better results than SVMs with HOG-descriptors.

Introduction

Digital cameras are used in a large variety of scientific and industrial applications. For most applications the acquired data should represent the real light intensity per pixel as accurately as possible. However, digital cameras are subject to different sources of noise which distort the resulting image. Noise includes photon noise, fixed pattern noise and read noise. These noise sources are dependent on various camera parameters, for example exposure time or sensor temperature. The aim of the radiometric calibration is to improve the quality of the resulting images by reducing the influence of the various types of noise on the measured data.

A commonly used calibration technique to remove noise is the flat field correction, also referred to as flat fielding. By assuming a linear pixel characteristic flat field correction corrects the pixel-to-pixel sensitivity. Flat field correction does not reflect the non-linearity of the dark current behavior or the full-well capability. Additionally, the ability to include random noise such as photon shot noise in the calibration process is very limited when using this classical method.

To take account of the non-linear pixel behavior, regression methods which allow for more flexible modeling should be used. Regression models estimate the correct intensities of the image pixels based on observed intensities and known camera parameters. One method that can be used is Gaussian processes regression – a supervised and non-parametric machine learning technique – which allows for modeling the characteristic of individual

pixels or groups of pixels dependent on various camera parameters. Gaussian processes are used because they adapt well to non-linear data which is under Gaussian noise. Additionally, only a few hyperparameters need to be optimized which can be done with gradient based optimization.

More precisely, Gaussian processes are used to model the mapping from exposure time and sensor temperature to real light intensity based on training data. This data should cover all achievable values of these three image parameters. In calibration, the real light intensity can be predicted for each pixel based on the trained regression model. Due to the computational complexity, standard Gaussian process regression is not suitable for applications which require a fast calibration.

We present a new approach for the calibration of digital cameras using sparse Gaussian processes. The sparse regression approach allows for faster training and calibration. Sparse Gaussian process regression uses a set of pseudo-inputs as additional parameters. These pseudo-inputs are derived from the original training data. The aim is an approximation for the complete training data set.

Using one regression model for each pixel raises high computational costs. Therefore the data needs to be split into a meaningful subset. The resulting quality as well as the required computation time for training are dependent on this step. We evaluated three different methods (1) one regression model per pixel, (2) one global regression model over all available images and (3) one regression model per cluster.

For our experiments we use a data set of images (256 images, each having 10 megapixels) sampled in equal intervals of real light intensity, exposure time and sensor temperature. The results show that the per pixel and global data selection are not suitable for image calibration. Due to the large amount of data the per pixel method is not realizable without special hardware – per image, 10 million regression models need to be trained. The global data selection makes the assumption that pixels at the same geometric location have equal characteristics. This is only true for some noise sources such as vignetting. Other noise sources (e.g. dark current and dirt or dust on the optical device) are not included in this model. For the final approach, pixels with equal characteristic are grouped into clusters. The characteristic of a pixel is defined by pixel value, exposure time and sensor temperature. Since in each cluster the behavior of all pixels is similar it is sufficient to take only one representative pixel per cluster over all images for training. For each cluster an individual Gaussian process regression and model selection is done. Calibration is performed by interpolating the gray-scale value of each pixel with the regression model of the respective cluster.

The experimental results show that calibration with sparse Gaussian processes is more accurate compared to classical flat field correction. We achieve a consistently higher reconstruction quality for the same overall number of calibration frames. In addition the calibration is faster than the standard Gaussian process approach. Important parameters for the proposed algorithm are the number of clusters and number of pseudo-inputs. The number of clusters can be set according to the camera system used. It influences data selection time and training time as well as the quality of the results. A lower number of pseudo-inputs results in faster training and calibration but a lower reconstruction quality.

Bibliography

- [1] Masaaki Tsujitani and Yusuke Tanaka. Cross-validation, bootstrap, and support vector machines. *Advances in Artificial Neural Systems*, 2011.
- [2] Tran Son Hai, Nguyen Thanh Thuy, et al. Image classification using support vector machine and artificial neural network. *International Journal of Information Technology and Computer Science (IJITCS)*, 4(5):32, 2012.
- [3] Navneet Dalal and Bill Triggs. Histograms of oriented gradients for human detection. In *Computer Vision and Pattern Recognition, 2005. CVPR 2005. IEEE Computer Society Conference on*, volume 1, pages 886–893. IEEE, 2005.
- [4] Alex Krizhevsky, Ilya Sutskever, and Geoffrey E Hinton. *ImageNet Classification with Deep Convolutional Neural Networks*, 2012.
- [5] Patrick Mutter. *Automatische Bestimmung von Kontextinformationen aus Bildern mit maschinellem Lernen*, 2016.
- [6] Alex Krizhevsky and Geoffrey Hinton. *Learning multiple layers of features from tiny images*, 2009.
- [7] Matthias Hermann. *Methoden des Deep Learning im Bereich Convolutional Neural Networks*, 2015
- [8] Yann LeCun. https://www.reddit.com/r/MachineLearning/comments/25lnbt/ama_yann_lecun/chizd8g, 23.03.2016
- [9] Nitish Srivastava, et al. Dropout. A simple way to prevent neural networks from overfitting, 2014.

Multi-resolution 3D Mesh Processing

Julian Schneider, Pascal Laube and Georg Umlauf

Based on pyramidal multi-resolution methods for mesh processing we propose a separation of surface detail and surface base geometry. We use subdivision as well as simplification of irregular meshes to extract mesh frequencies. By enhancing or reducing certain mesh frequencies one can apply signal like filtering to 3D meshes.

Introduction

Pyramidal multi-resolution methods are an important tool of signal processing. Their application to irregular 3D meshes is strongly based upon subdivision and simplification. By applying a so called relaxation step and subsequent subdivision one can compute a mesh pyramid. We apply multi-resolution methods for separation of base geometry and surface detail.

Method

Relaxation as introduced by Guskov et al. [2] is the process of changing a vertex position so that surface curvature is minimized. Relaxation can be seen as a low-pass filter. Relaxation is done per edge by minimizing second order differences. Relaxation operator Rg_i is defined as

$$Rp_i = \sum_{j \in V_2(i)} w_{i,j} p_j \quad (1)$$

with vertex v_i positioned at p_i and relaxed position Rp_i with

$$w_{i,j} = - \frac{\sum_{e \in E_2(i)} |j \in w(e)| c_{e,i} c_{e,j}}{\sum_{e \in E_2(i)} c_{e,i}^2}. \quad (2)$$

Here $V_2(i)$ is the 2-ring neighbourhood with flaps of vertex v_i . The $w_{i,j}$ are weights in the process of relaxation. The $c_{e,i}$ depend on geometric positions of mesh vertices in the 2-ring.

This concept has been further improved by Roy et al. [3]. They use the Meyer differential operator for curvature relaxation.

They compute $w_{i,j}$ as

$$w_{i,j} = - \frac{\cot(\alpha_{i,j}) + \cot(\beta_{i,j})}{\sum_{l \in V_1(i)} \cot(\alpha_{i,l}) + \cot(\beta_{i,l})} \quad (3)$$

This relaxation operator is based not on the 2-

ring neighbourhood but the 1-ring neighbourhood of v_i .

$$Rp_i = \sum_{j \in V_1(i)} w_{i,j} p_j \quad (4)$$

Additionally to this relaxation a sub-sampling process is applied after each relaxation step. Based on so called edge-collapses the mesh topology is simplified. This simplification is part of an the progressive mesh algorithm by Hoppe et. al. [3].

By applying this methodology one can now apply different filters to an original model (Fig.) like a lowpass filter (Fig.), a stopband filter (Fig.), or even enhancement filters (Fig.).

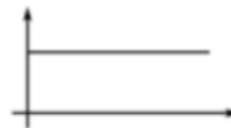


Figure 17: Original model.



Figure 18: Lowpass filter.

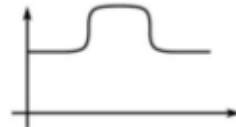


Figure 20: Enhancement filter.



Figure 19: Stopband filter.

Bibliography

- [1] Roy, Michael, et al. "Multiresolution analysis for irregular meshes." *Wavelet Applications in Industrial Processing*. Vol. 5266. International Society for Optics and Photonics, 2004.
- [2] Guskov, Igor, Wim Sweldens, and Peter Schroeder. "Multiresolution signal processing for meshes." *Proceedings of the 26th annual conference on Computer graphics and interactive techniques*. ACM Press/Addison-Wesley Publishing Co., 1999.
- [3] Hoppe, Hugues. "Progressive meshes." *Proceedings of the 23rd annual conference on Computer graphics and interactive techniques*. ACM, 1996.

3D Primitive Classification Using Stacked Autoencoders

Merlin Blume, Pascal Laube, Matthias O. Franz, Oliver Deussen & Georg Umlauf

This work is dedicated to the recent developments in the field of deep learning. Focusing specifically on the discipline of unsupervised representation learning, five different types of regularized deep autoencoders have been evaluated on their 3D object classification capabilities. While each autoencoder scored with a positive classification rate of above 99%, convolutional neural networks initialized by autoencoders achieved the best score with 99,8%. The used training data contained six different types of primitives (planes, cylinders, cones, spheres, ellipsoids and tori) with varying parametrization and arbitrary transformations per object. Because there is a lack in publicly available labeled point cloud data, each primitive needed to be sampled synthetically. Finally three visualization techniques were implemented to qualitatively inspect each autencoder's hidden layer weights. Their analysis revealed interesting structures similar to those in the domain of 2D computer vision.

The manufacturing process of complex entities (like cars or airplanes) involves many different stages within the construction cycle. One of the most important parts is the digital engineering phase supported by key technologies like CAD & CAE. Especially in case of organic free-form surfaces digital design and reverse engineering operate hand in hand. Although the discipline of reverse engineering is primarily known in the context of product piracy there are many serious applications making it indispensable in production, whether it be the reconstruction of lost digital blueprints, the use of rapid prototyping with clay models or quality assurance matching manufactured parts against their digital copy.

In addition 3D scanning procedures have become more precise, faster and even cheaper. During the scanning, which can be based on contact sensors or optical systems, numerical data describing discrete 3D positions get sampled. The resulting Cartesian pointclouds serve as primary product for the reproduction of digital assets. This is where it gets tricky. Lots of algorithms have been developed for the extraction of approximating meshes. The conversion to mathematical surface descriptions however still depends very much on manual fine-tuning.

We attempt the experiment to go one step further in the direction of process automation. Therefore we will make use of modern concepts related to the field of machine learning. Within the last years the buzzword "big data" gained lots

of attention. It is describing nothing less than a change in paradigm in our information-driven society. The trend departs from the pure analytical approach to the examination of huge databases. The amount and quality of data, but also nowadays computational power make a variety of new applications possible. Using intelligent systems, the manufacturing industry can benefit from the latest developments as well. Such algorithms learn autonomously and can easily adapt to unseen new data. Focusing on reverse engineering we will explore a method to detect and classify primitive shapes for the later extraction of mathematical bodies.

The discipline of deep learning lately gained a lot of interest in diverse fields of application. While its popularity and the fast evolvement of new techniques is quite desirable, it also raises the entry hurdle for inexperienced scientists at the same time. As a consequence one of our primary goals was to establish a good understanding for deep learning and some of the fundamentals one requires to fully grasp the overall challenges that go along with machine learning. Focusing on the automatic, unsupervised extraction of concise features for the classification of 3D primitives we turned our attention towards the field of representational learning, exclusively working on various implementations of autoencoders. Therefore we explored up to five types of autoencoders (AEs) and analysed their different approaches to model regularization.

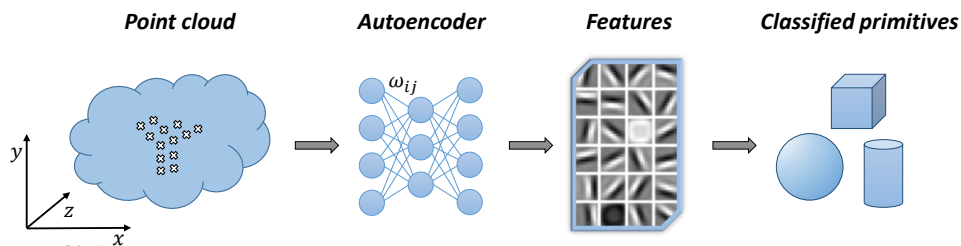


Figure 21: Compared to conventional methods autoencoders extract features automatically based on raw data. These features in turn build the foundation for final classification.

The first step to our experiments was the acquisition of training data. We generated a set of 50,000 randomly affine transformed pointclouds. As always with machine learning, data preprocessing was of mayor importance, since all point clouds varied in their number of samples and didn't possess any intrinsic consistent structure. To overcome this problem we decided to voxelize each point cloud generating regular rectangular grids. Normalizing the count of embodied points within each cell to a value in the range of $[0, 1]$ our object representation provided a 3D equivalent to 2D grayscale images. While the voxelization step led to transition and uniform scaling invariance, it did not eliminate the effect of arbitrary rotations. Experimenting with PCA and the objects' moment of inertia, we were able to sufficiently well align objects of the same type. However, to accommodate the idea of raw data processing without the slightest induction of expert knowledge, we decided to abstain from this reorientation.

The comparison with established machine learning procedures like Naive Bayes, Linear Discriminant Analysis and SVMs allowed us to better judge our experiments' outcomes. SVMs achieved high classification rates, even though grid search

took them a long time to find a good initialization. Limited by the number and complexity of experimental setups we still succeeded in discovering topological structures and working parametrization for all deep models. The classification with stacked AEs always surpassed our baseline scores.

In a final step we tried to judge the performance of our AEs intuitively. For this we analysed for each model a limited set of hidden layer weights visually. Hoping to identify relevant features and to raise confidence in the methods applied, we found significant structures within the weights' graphical representations. Unfortunately they didn't allow us to fully understand what happens inside the AEs networks. Even though the features must be of importance to the machine learner, they seem to elude the visual perception of humans. Nevertheless we could spot some interesting patterns like the very frequent appearance of kidney shaped features. Considering the nature of our data and the object types they predominantly occurred with, we assume that such "kidney filters" might represent a match to 2D edge detectors. However it will take more research to check, if our interpretation is reasonable.

Vector Machines for Knot Placement in B-Spline Curve and Surface Approximation

Pascal Laube, Georg Umlauf, Matthias Franz

Knot placement for curve and surface approximation is an open problem. Selecting knot values to receive good approximation results is a challenging task. Proposed approaches range from parametric averaging to genetic algorithms. We propose the use of Support Vector Machines (SVMs) for finding suitable knot vectors in B-spline curve approximation. The SVMs are trained to be able to distinguish between locations along the curve that are well or not well suited as knots in the parametric domain. This score is based on different geometric features of a parameters corresponding point in the point cloud. A score weighted averaging technique is used to produce the final knot vector. We further propose a method to use the score weighted averaging technique for T-spline surface approximation.

Finding a good knot vector for curve and surface approximation is a common problem in many applications like e.g. Reverse Engineering (RE). In RE one starts with a sampled physical object represented by a point cloud. For this point cloud a corresponding CAD representation must be recovered. After steps such as pre-processing and segmentation, a B-spline approximation of the point cloud or parts of it is computed. For this approximation the data points, parameter values for the data points, the B-spline degree, and an appropriate knot vector are required. Then the goal is to generate knot vectors that lead to approximations with as little deviation from the data set, for as few knots as possible. Usually a certain threshold has to be satisfied to assure a sufficient approximation quality. Since the number of control points is determined by the number of knots, the number of knots is especially important if the resulting curves and surfaces will be further processed by a human operator.

Because there are many unknowns in the approximation process, we propose knot vector computation using machine learning methods. We train Support Vector Machines (SVMs) to distinguish between locations along a curve that are well or not well suited as knots in the parametric domain. For training and classification we use a feature vector that concentrates information about a point clouds geometric structure. Consider a set of ordered points in two dimensional space. We define a good knot vector as the one that generates little deviation to the data set while having a small number of knots. Finding the ideal knot vector is impossible. A computationally very expensive way is to exhaustively search for appropriate

knot value combinations in the set of parameters. Due to computational cost this is not feasible for practical application. Since training data has to be generated only once the cost of exhaustive search in our case is negligible. After training the SVMs are able to assign a score to each point of a point cloud based on its local point neighborhood.

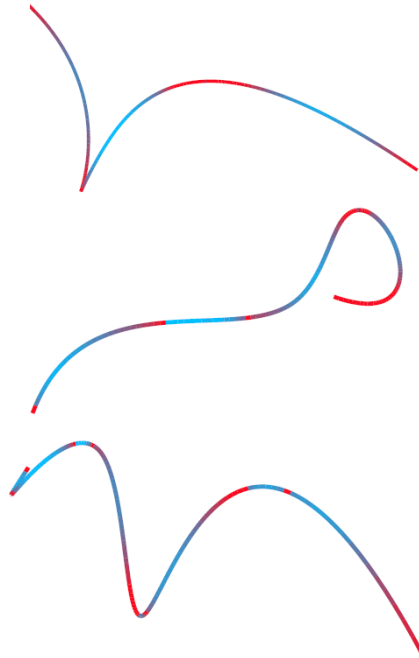


Figure 22: Three exemplar curves colored by score from high score (red) to low score (blue).

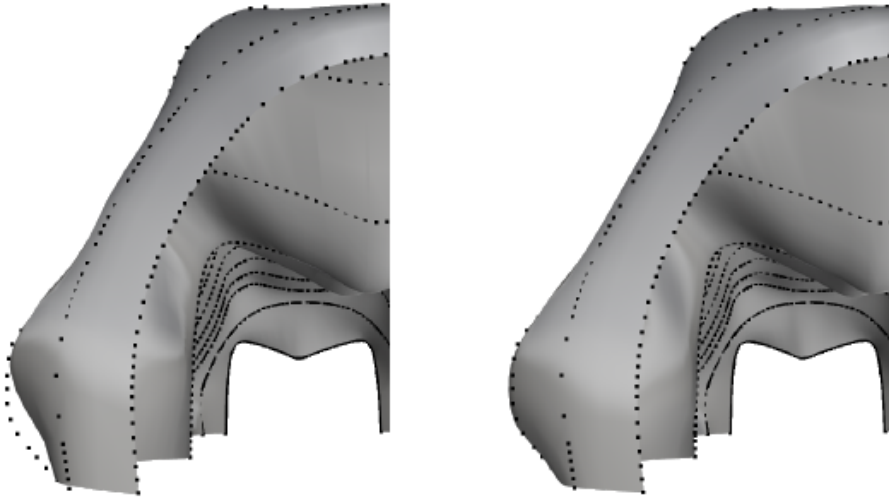


Figure 23: T-spline surface approximation by NKTP on the left and by SWKP on the right together with the original point data.

An score-weighted averaging yields then the final knot vector. This concept for B-Spline curve approximation is then applied for T-spline surface approximation. B-spline surface interpolation by surface skinning or lofting is the process of interpolation by contour curves (CCs). For an ordered set of points in which each point belongs to a serial contour along the surface one has to first interpolate points along CCs. The compatibility of the CCs needs to be ensured by degree elevation to a common degree. By interpolating the CCs one receives the lofted surface. Approximation of CCs results in an approximate lofted surface. Unordered sets of points can be converted to ordered sets for surface lofting by point cloud slicing. We propose an approach for B-spline curve and T-spline surface approximation. We train SVMs to decide on the suitability of pre-computed parameter values of a point cloud as values for a knot vector. Based on this suitability measure, or score,

we perform a weighted averaging of parameter values to create the knot vector. This concept is further adapted for T-spline surface approximation by lofting. The proposed method produces approximations of good quality. This is especially the case for approximation with a small number of knots. We could show that SVMs are able to learn characteristics of positions along a curve where knot placement has positive impact on approximation quality. The approximation by lofted T-spline surfaces is able to preserve initial knot vectors of CCs and needs a fraction of the knots a comparable B-spline surface would need to satisfy a certain threshold. For future works we plan to investigate the applicability of machine learning to other steps of the RE process like point cloud segmentation. We further would like to apply deep learning techniques that render manual feature selection obsolete like e.g. neural networks with an auto-encoder layer.

A Virtual-Reality 3d-Laser-Scan Simulation

Malvin Danhof, Tarek Schneider, Pascal Laube, Georg Umlauf

We present a 3d-laser-scan simulation in virtual reality for creating synthetic scans of CAD models. Consisting of the virtual reality head-mounted display Oculus Rift and the motion controller Razer Hydra our system can be used like common hand-held 3d laser scanners. It supports scanning of triangular meshes as well as b-spline tensor product surfaces based on high performance ray-casting algorithms. While point clouds of known scanning simulations are missing the man-made structure, our approach overcomes this problem by imitating real scanning scenarios. Calculation speed, interactivity and the resulting realistic point clouds are the benefits of this system.

In science and industry 3d laser scanners are widely used to acquire 3d point data of real world objects. The result of a scanning process is a 3d point cloud. Often a CAD representation of these point clouds needs to be recovered for the subsequent processing. This task is performed by the reverse engineering process. Thus, the quality of the CAD representation depends on the chosen reverse engineering process.



Figure 24: FARO Edge ScanArm (www.faro.com, 09/25/2015)

Evaluating reverse engineering algorithms is only possible if a large set of point clouds is available. To acquire these point clouds CAD models are scanned virtually. There are two reasons for this approach. First, we often lack enough suitable physical objects to scan and, second, point clouds of hand-scanned physical objects often lack corresponding CAD information. However, point clouds of hand-scanned physical objects and synthetically generated point clouds differ heavily in their structure in terms of scan-strategy and scan-path. Since each human operator has a different scan-strategy and scan-path, the resulting point clouds

differ much in structure, even if the same object was scanned. On the one hand this structure is not completely random, on the other hand there is no good model for the human scanning procedure. For a fair evaluation of reverse engineering algorithms with realistic data this man-made structure must be incorporated into the data. To generate scans of CAD models that capture this man-made structure we propose a virtual reality (VR) scanner setup. We present a method to generate 3d point clouds from CAD models consisting of triangle meshes and b-spline tensor product surfaces with a simulated hand-held laser scanner in a VR environment (Fig. 25).



Figure 25: VR setup.

Our goal is to create a realistic simulation of the scanning process with a hand-held laser scanner like the FARO Edge ScanArm (Fig. 24). Using this approach we can compute 3d point clouds of CAD models using a virtual laser scanner with a man-made scan structure.

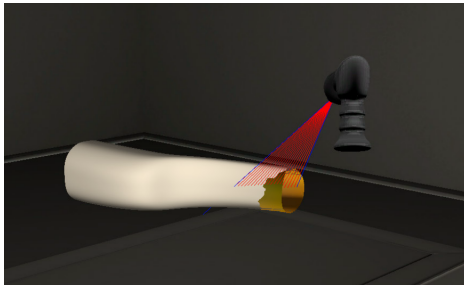


Figure 26: The virtual scene.

For the simulation of a hand-held 3d laser scanner we propose a VR environment. The structure of the synthetic point clouds generated in this VR is similar to man-made scans of physical objects due to the manual scanning process. The virtual scene consists of a workshop with a table, that carries the CAD model, and a virtual model of the scanner, see Figure 26. The user can move freely in the scene, change the perspective and field of view in terms of the CAD model and operate the laser scanner. For the VR setup two essential peripherals are used: the VR headset Oculus Rift for visual immersion and the motion controller Razer Hydra for scanner control and scene navigation. The Oculus Rift provides a 3d view of the VR scene and allows to freely explore the 3d scene. Integrated sensors provide data about the user's head position and orientation. Due to its large

field of view the degree of immersion in the scene is very high. The Razer Hydra consists of two wired controllers and a base station, which creates a magnetic field to determine the controllers' spatial positions. It can capture hand movements and orientations accurately and provides joysticks and buttons for control tasks. Both devices are integrated using the manufacturer' APIs: Oculus Rift SDK and Sixense Core API.

This solution makes scanning of CAD models inside a VR environment possible. Interaction with our system matches the process of operating a real hand-held laser scanner. The resulting point clouds cannot be differentiated from non-synthetic scans. Interactivity and execution speed of our application meet the expectations. The scan process is realistic and easy to perform. Nevertheless there are a few drawbacks. The Razer Hydra is not connected to a leading arm like some real laser scanners which leads to difficulties moving the scanner calm and precise. This could be compensated by an adjustable factor which decreases the sensitivity of the Hydra. Since the Oculus Rift is still in development there are a few points which will certainly improve with later versions. Especially the resolution causes the problem of a visible pixel grid and a blurry perception of concrete shapes on looking around in a scene. This problem will hopefully get fixed with newer versions which should have a higher pixel density.

Morphed 3d fish models using multi-perspective 2d fish images

Leonard Thiessen, Pascal Laube, Ulrike Siebeck and Georg Umlauf

In this work we present a method to generate 3d fish models based on 2d fish images. First 3d and 2d contours are extracted. Then correspondences are computed and the shape of the 3d model is morphed, using a spring-mass system, to the 2d reference contour. 3d vertex coordinates are interpolated to yield the final 3d fish model.

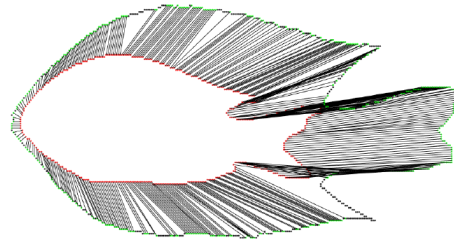
Introduction

Based on the long-standing research cooperation of the HTWG Konstanz, in particular the Institute of Optical Systems, and the Faculty of Biology of the University of Brisbane, joint research projects take place regularly. The aim of the research project "Fishmorph" is to generate lifelike reconstructions based on image data, 3D data and sample models of various fish to be able to realistically map the ichthyological conditions at the Great Barrier Reef on the endemic species there. In order to be able to receive the partially species-protected fish, the fish must be measured alive and then reset. The 3d reconstructions will be used in further projects to investigate the behaviour of fish. In recent years the research in the field of behavior and perception for fishes has been insightful. It has been discovered, that particular species of reef fish are able to detect simple and complex shapes as shown in [3], and that these fishes can also use ultraviolet light to detect other fishes [2]. And as recently shown in [4] the archerfish has the capability to discriminate human faces. This is remarkable, because this ability is attributed to the cortex, but a fish has no cortex.

Another interesting research purpose for 3d reconstructions is the perception of fishes, especially the way how a fish perceives other fishes and what the crucial point are, where a fish recognizes another fish as a predator or another harmless fish. Discovering this behavior requires experiments with fishes. Here one problem is that some of the fishes are endangered, but they have proven as relevant for this kind of research. This could be avoided by usage of an animation for such experiments as proposed in [5]. The usage of computer animations or 3d models in such a research field is already ongoing. In [4] 3d models of human faces were used for this experiment. So 3d models of fishes could support the current research purposes. The problem remains, that there are no accurate fish models.

Method

The focus of this work was to generate new 3d models of fishes based solely on texture images. Therefore, a 3d prototype model for each desired fish species or family is required and the images should show the respective fish from different perspectives, since one image can only model one perspective. Out of these different perspective we extract the fishes shape (or contour).



A 3d fish prototype model will then be adapted (or morphed) to match the fishes reference shapes. Shape matching is applied to discover correspondences between the contour of the 3d model and the 2d reference contours which allows to adapt the contour of the model to the reference's contour. Morphing the 3d model is done by applying a mass-spring system in image space and then interpolating 3d vertices with regard to the morphed pixels. The mass-spring system determines where which parts of the prototype model should be moved to, to generate a 3d model that looks like the reference fish. This process has to be repeated several times for each fish perspective to get an accurate 3d model in the end.

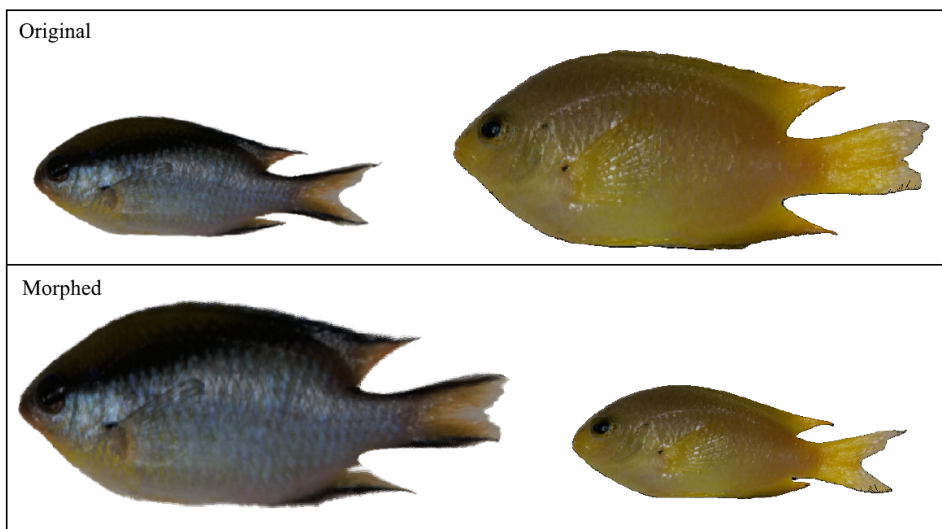
Conclusion

We could show, that the approach of a texture-based deformation of 3d models, is able to produce accurate 3d fish models. The 2d/3d morphing achieved results which can be used for research

purposes in the field of behavioural research of fishes. Obviously the results are heavily depending on the input data and especially contour extraction and contour matching. For future work we plan to introduce a 3d mass-spring system which is able to preserve the 3d models volume to counteract volume degeneration.

Bibliography

- [1] Cai, Jian-Feng and Chan, Raymond H and Shen, Zuowei: A framelet-based image inpainting algorithm. *Applied and Computational Harmonic Analysis*, 24, 131–149, 2008.
- [2] Siebeck, U. E., Parker, A. N., Sprenger, D., Maethger, L. M., and Wallis, G.: A species of reef fish that uses ultraviolet patterns for covert face recognition. *Current Biology*, 20(5), 407-410, 2010.
- [3] Siebeck, U. E., Litherland, L., and Wallis, G. M.: Shape learning and discrimination in reef fish. *Journal of Experimental Biology*, 212(13), 2113-2119, 2009.
- [4] Newport, C., Wallis, G., Reshitnyk, Y., and Siebeck, U. E.: Discrimination of human faces by archerfish (*Toxotes chatareus*). *Scientific reports*, 6, 27523, 2016.
- [5] Woo, K. L., and Rieucau, G.: From dummies to animations: a review of computer-animated stimuli used in animal behavior studies. *Behavioral Ecology and Sociobiology*, 65(9), 1671, 2011.



On-line splat rendering

Marco Fehrenbach, Korkiat Khumphai, Felix Schuckert, and Georg Umlauf

Scanning real objects with the Faro Edge 3d ScanArm produces a large amount of geometrical points. Additionally during the scanning process the point cloud is able to grow dynamically or to replace a large area of points. The reconstruction of these points is very time consuming. To render a valid representation of the real object, we implemented a splat rendering process. The process uses the GPU to display the point cloud in real time. With this process the user is able to see the scanning results immediately.

Introduction

Scanning real objects is an important topic of computergraphics. An use case is to reconstruct the real object in a CAD representation. Another case is to identify the scanned object with the help of machine vision and learning. Nowadays the used hardware is very accurate and produces a large amount of useful data. For example the used Faro Edge 3d ScanArm. But the representation of the data is either very time consuming or needs additional interpretations. The solution is the implementation of a splat rendering process. The process directly uses the raw input data without any precomputations or additional requirements. Also it can handle the dynamic behaviour of the input data during the scan process. The result implementation is a part of an existing project to reconstruct CAD geometry [1].

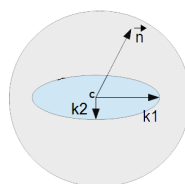


Figure 27: A single splat with the mathematical definitions

To render a large amount of points, we used an accelerating control structure. Because the input points don't move, we choose an octree implementation. The octree uses the OpenGL vertex buffer objects to send the data to the GPU. Each leaf in the tree includes a single buffer object with configurable size. If a point is added to or removed from a leaf, the octree rebuilds a single vertex buffer only. This structure is able to support frustum culling on the CPU and to reduce the workload between the main memory and the GPU memory. See figure ?? for a culling example.

Splat rendering process

The splat rendering process is based on the previous work of Botsch et. al. [2]. It uses the technique to expand the point size of the OpenGL pipeline. Then the normal of the point is used to discard single pixels of the point sprite. The sprite matches a rotated ellipse, which represents the surface at the point position. See figure 27. The gray circle represents the original sprite. C is the original point and \vec{n} the surface normal. Additionally, to calculate the phong lighting model, the main curvatures $k1$ and $k2$ and the directions are needed. The blue ellipse represents the result pixels to draw.

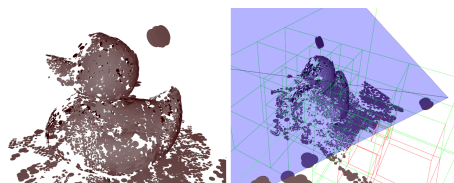


Figure 28: Left: Original camera image, right: Frustum in blue with rendered leaves in green and culled leaves in red.

Results

We used a couple of objects to validate the result of the implemented splat renderer. Figure 29

shows an elephant toy scanned with our Faro laser scanner. The point cloud includes approximately 100.000 points.



Figure 29: Representation of an elephant toy with approximately 100.000 splats.

Also the figure shows the different scanning qualities. The abdominal area doesn't contain enough points to represent the surface completely. In contrast to the head. The difference is due to the behaviour of the user. So the user can see, which area needs more input data to be complete. The performance of the algorithm depends on the number of input data, the size of the splats and the used GPU. Because the fragment shader gets the most load in the program, using a small splat

size with more points is very effective. For a few points, using a large splat size can create an invalid surface representation. See figure 30.

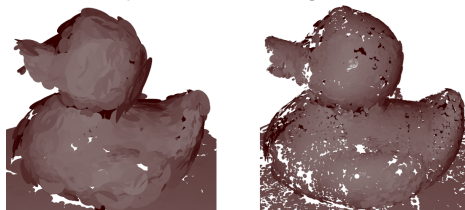


Figure 30: Representation of a duck with different number of splats and splat sizes.

Bibliography

- [1] Denker, K. and Hagel, D. and Raible, J. and Umlauf, G. and Hamann, B.: On-line Reconstruction of CAD Geometry, Inter. Conf. on 3D Vision, 151-158, 2013.
- [2] Mario, Botsch and Michael, Spornat and Lief, Kobbelt: Phong Splatting, Computer Graphics Group, RWTH Aachen Technical University, 2004, Presented on Eurographics Symposium on Point-Based Graphics.

Energieeffiziente Beleuchtung von Solitärobjekten

Fatih Demiralp, Gero Kern, Melanie Walde, Bernd Jödicke

Allein die Dosis macht das Gift. Was schon Paracelsus in Bezug auf Medizin feststellte, lässt sich auch ohne Weiteres auf das Thema Licht übertragen. Dies lässt sich unschwer beim Betrachten exzessiver Solariumgänger beobachten. Die richtige Dosis ist auch Untersuchungsgegenstand dieser Publikation. Wie viel Licht ist ausreichend, um ein Solitärobject sowohl energiesparend zu beleuchten, als auch aufmerksamkeitswirksam von seiner Umgebung abzuheben. Das Ziel dieser Projektarbeit ist die Ermittlung der optimalen Leuchtdichte, um obigen Anforderungen gerecht zu werden.

Für den Versuch wurde ein Objekt mit unterschiedlich viel Licht beschienen. Die Qualität der erzeugten Beleuchtungen wurde dann bewertet.

Als zu beleuchtendes Objekt wurde die Riesenbergkapelle in Konstanz ausgewählt. Diese eignet sich für den Versuch besonders gut, da sie sich auf der lichten Spitze eines bewaldeten Hügels befindet. Zum einen ist sie frei vom störenden Einfluss künstlicher Lichtquellen, zum anderen können die verschiedenen Beleuchtungen aus großer Distanz beobachtet und bewertet werden.

In der konkreten Umsetzung lief der Versuch wie folgt ab: Als Lichtquelle wurde eine auf einen Wertebereich zwischen $0,03 \sim cd/m^2$ und $3 \sim cd/m^2$ dimmbare LED-Leuchte verwendet. Insgesamt wurden drei Messreihen durchgeführt. Eine Messreihe umfasste fünf verschiedene Beleuchtungsintensitäten. Bewertet wurden die verschiedenen Beleuchtungsszenarien von einem Zwei-Mann-Team von einem $700 \sim m$ entfernten Standort aus. Zur Bewertung wurden Zensuren von eins bis vier vergeben. Ursächlich für eine schlechte Zensur kann sowohl eine zu geringe Leuchtdichte sein, bei der das Objekt als zu dunkel wahrgenommen wird, als auch eine zu hohe Leuchtdichte, bei der die Objektfläche blendend wirkt. Als Messwerte wurden sowohl die Leuchtdichte L als auch die Beleuchtungsstärke E ermittelt.

Abbildung 1 veranschaulicht die unterschiedlichen Beleuchtungsintensitäten. Sie sind der persönlichen Wahrnehmung nachempfunden dargestellt.

Das Ergebnis des Experiments (Abbildung 2) zeigt, dass sich bei $0,3 \sim cd/m^2$ ein eindeutiges Maximum einstellt. Bei dieser Leucht-

dichte wird die Objektbeleuchtung als besonders angenehm empfunden. Eine Leuchtdichte von $0,82 \sim cd/m^2$ wird als zu hell und fast schon blendend wahrgenommen. Werte unterhalb einer Leuchtdichte von $0,1 \sim cd/m^2$ werden als zu dunkel bewertet. Verglichen mit dem unbeleuchteten Zustand hebt sich ein Objekt selbst bei einer Leuchtdichte von $0,03 \sim cd/m^2$, immer noch sichtbar von seiner Umgebung ab. Die Leuchtdichte ist jedoch nicht ausreichend, um Aufmerksamkeit auf das Objekt zu ziehen. Der Bereich um $0,1 \sim cd/m^2$ stellt einen guten Kompromiss zwischen Energieeffizienz und Inszenierung dar.

Bei der Objektbeleuchtung spielt neben dem gewählten Leuchtmittel und der Intensität auch das Material eine entscheidende Rolle. Eine wichtige Kennzahl in diesem Zusammenhang ist der Reflexionsgrad ρ der Objektfläche. Dieser lässt sich aus der Beleuchtungsstärke E und der Leuchtdichte L bestimmen:

$$\rho = \frac{L \cdot \pi}{E}$$

Beim Untersuchungsobjekt beträgt der Reflexionsgrad 55%, dabei handelt es sich um eine Fassade aus weißem Putz. Die Größe des Objekts und das gewählte Leuchtmittel bzw. dessen Lichtausbeute η sind entscheidende Parameter bei der Berechnung der notwendigen elektrischen Leistung P . Diese lässt sich unter Zuhilfenahme der Beleuchtungsstärke E und der Fläche A wie folgt berechnen:

$$P = \frac{E \cdot A}{\eta}$$

Am Beispiel der 30 m^2 großen beleuchteten Front des Solitärobjects ergibt sich bei Verwen-

dung von LED-Leuchten mit $\eta > 100lm/W$ am Optimalpunkt ($\emptyset 0,3 cd/m^2$ bzw. $1,7 Lux$) ein Leistungsbedarf von rund $0,5 W$. Unter Berücksichtigung möglicher Verluste empfiehlt es sich, von einer Leistung von mindestens $1 W$ auszugehen. Voraussetzung hierfür ist, dass die zu beleuchtende Fläche und der Reflexionsgrad dem Untersuchungsobjekt entsprechen.

Die technische Umsetzung des Beleuchtungskonzepts kann dabei kostengünstig durch die Verwendung einer solarbetriebenen Leuchte erfolgen. Hierbei wird im Laufe des Tages ein Akku geladen, mit dem dann über die Nacht die LEDs betrieben werden. Der weitestgehend autarke Betrieb ermöglicht selbst bei sehr abgelegenen Objekten ohne Netzzugang eine optisch ansprechende Inszenierung.

Um ein Solitärobjekt optimal zu beleuchten wird eine Leuchtdichte von $0,3 cd/m^2$ vorgeschlagen. Die ermittelten Werte gelten aufgrund der

geringen Anzahl an Messreihen und der bewertenden Personen nur als grobe Orientierung. Weitere Versuche zur Validierung der Ergebnisse erscheinen sinnvoll.

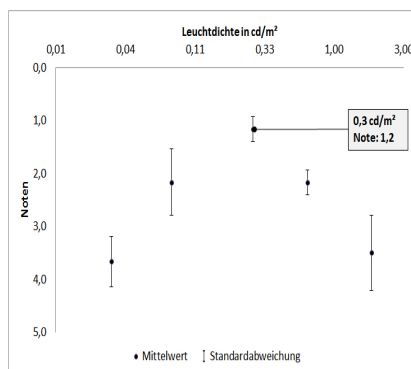


Figure 31: Untersuchungsergebnisse.

Melanopische Lichtwirkung - Aktuelle Erkenntnisse aus Forschung und Lichtplanung

Daniel Feuser, Gabriela Guillen und Thomas Scheiling

Licht und dessen biologische Wirkung ist schon seit mehreren Jahren ein wichtiges Thema. Einige namhafte Firmen sprechen sogar von der dritten Dimension des Lichts. Dennoch dürfen Begriffe wie biologische Lichtwirkung und melanopische Lichtwirkung nicht synonym verwendet werden. Dieser Artikel gibt einen Überblick über die wissenschaftlichen Grundlagen zum Thema *melanopische Lichtwirkung* und liefert erste Ansätze für eine konkrete Umsetzung in der Lichtplanung.

Licht ist für den Menschen unverzichtbar. Es verhilft uns nicht nur zum Sehen, es hat auch Auswirkungen auf unser Wohlbefinden und die Gesundheit. Unsere sogenannte "innere Uhr" wird täglich durch das Tageslicht synchronisiert und übernimmt daraufhin wichtige Steuerungsaufgaben im Körper.

Das Leben des modernen Menschen findet heute nicht mehr maßgeblich im Freien sondern überwiegend in geschlossenen Räumen mit künstlicher Beleuchtung statt. Der positive Einfluss von Tageslicht verringert sich dadurch immer mehr. Fehlt das Tageslicht, so gerät die innere Uhr aus dem Takt, was zu Schlafstörungen, chronischer Müdigkeit und im schlimmsten Fall zu Depressionen führen kann.

Tageslicht zeichnet sich insbesondere durch sein Spektrum und seine Dynamik aus. Am Morgen und am Abend, d.h. während des Sonnenaufgangs und des Sonnenuntergangs, verschiebt sich das Spektrum zu einem erhöhten Rotanteil. In der Zeit dazwischen enthält das Tageslicht einen erhöhten relativen Anteil am blauen Spektrum.

Im Jahr 2001 entdeckten Wissenschaftler spezielle Ganglienzellen auf der Netzhaut. Im Gegensatz zu den bekannten Stäbchen und Zapfen unterstützen diese jedoch nicht das Sehen, sondern vermitteln nicht-visuelle Reize an das Gehirn und steuern damit biologische Vorgänge im Körper [2]. Zu den nachgewiesenen Vorgängen zählen unter anderem [1]:

- Die Unterdrückung der Melatonin-Produktion
- Die Stabilisierung der inneren Uhr
- Die Steigerung des Wachheitsgrades

Diese speziellen Fotorezeptoren arbeiten mit dem Photopigment *Melanopsin* und reagieren äußerst sensibel auf Licht im blauen Spektrum. In der Fachliteratur werden lichtinduzierte biologische Vorgänge als *melanopische Lichtwirkung* bezeichnet. Diese Entdeckung verleiht der Thematik Licht eine neue Dimension. Zur eigentlichen Sehaufgabe kommt ein gesundheitlich-biologischer Aspekt hinzu, der in den letzten Jahren zunehmend diskutiert wurde. Eine *melanopisch wirksame* Beleuchtung orientiert sich am Tageslicht und bringt dadurch zusätzlich zur visuellen eine nicht-visuelle Wirkung mit sich. Eine solche Beleuchtung soll sich den jeweiligen Bedürfnissen des Menschen anpassen. Zusätzlich zur Stabilisierung der inneren Uhr wird das Leistungsvermögen und die Konzentration in den aktiven Phasen gesteigert und eine nachhaltige Regeneration in den Erholungsphasen begünstigt [2].

Melatonin Suppression

Das Epiphysenhormon *Melatonin* wird in den Nachtstunden im Gehirn produziert. Es fördert die Müdigkeit und kann durch seine Ausschüttung die innere Uhr beeinflussen.

Licht einer gewissen Wellenlänge und Beleuchtungsstärke ist in der Lage die Melatonin-Produktion zu unterdrücken bzw. zu vermindern. Abbildung 32 zeigt die spektrale Empfindlichkeit der Melatonin-Suppression gegenüber der bekannten spektralen Hellempfindlichkeit $V(\lambda)$. Der Punkt der größten Empfindlichkeit befindet sich bei ca. 450 nm und ist damit, verglichen mit der spektralen Hellempfindlichkeit $V(\lambda)$, ins blaue Spektrum verschoben. Eine licht-induzierte Melatonin-Unterdrückung kann folglich nur bei

einer Strahlung stattfinden, deren Spektrum die Wellenlängen zwischen 350 nm und 550 nm beinhaltet.

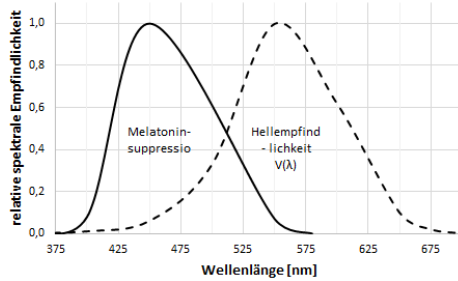


Figure 32: Wirkung monochromatischen Lichts auf die Melatonin-Unterdrückung in der Nacht verglichen zur spektralen Hellempfindlichkeit $V(\lambda)$ [14].

Zusätzlich zum richtigen Spektrum erfordert die Melatonin-Suppression eine geeignete Beleuchtungsstärke. "Inzwischen ergeben neueste Untersuchungen [...], dass die 50%-Wirkungsschwellen für melanopische Lichtwirkungen wie Melatonin-Suppression, [...] zwischen 90 und 180 lx vertikaler Beleuchtungsstärke am Auge liegen" [1]. Abbildung 33a) zeigt die Ergebnisse eines Versuchs, bei dem durch eine nächtliche 6,5 Stunden dauernde Exposition mit weißem Licht¹ und 100 lx vertikaler Beleuchtungsstärke der Melatonin-Gehalt im Blut vollständig unterdrückt wurde.

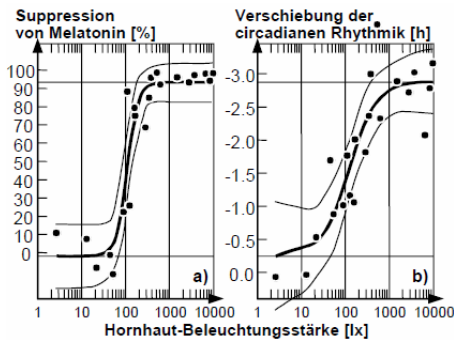


Figure 33: Lichtinduzierte Suppression von Melatonin und Verschiebung der circadianen Rhythmik auf der Zeitachse [6].

Für die Unterdrückung der Melatonin-Produktion sind jedoch noch weitere Faktoren entscheidend. So sollten zusätzlich zum Spektrum und der Beleuchtungsstärke auch die Dauer der Bestrahlung und die Richtung, aus der bestrahlt wird, erfasst und analysiert werden. Quellen bele-

gen, dass Licht, welches von oben ins Auge fällt, die Melatonin-Produktion wirksamer unterdrückt als Licht von unten [3]. Weitere Einflüsse wie intermittierendes Licht können den folgenden Quellen entnommen werden [4] [5] [8] [9].

Stabilisierung der inneren Uhr

Die innere Uhr, oder fachlich der circadiane Rhythmus, beschreibt einen biologischen Rhythmus mit einer Periodendauer von etwa 24 Stunden. Er steuert wichtige Funktionen im Körper, wie beispielsweise die Herzfrequenz, die Körpertemperatur oder den Schlaf-Wach-Rhythmus.

Licht ist einer der wichtigsten Taktgeber für die Synchronisation der circadianen Rhythmik auf die 24 Stunden eines Tages. Die Zirbeldrüse im Gehirn beginnt am Abend damit, Melatonin auszuschütten, wobei von zwei bis drei Uhr morgens der Höhepunkt erreicht ist und der Melatonin-Gehalt im Blut dann wieder absinkt (Abbildung 34).

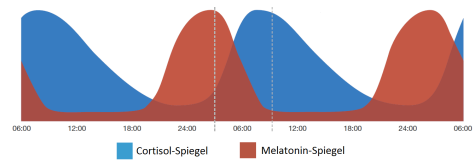


Figure 34: Beispielhafter Cortisol- und Melatonin-Verlauf [13].

Es ist nachgewiesen, dass geeignetes Licht zur richtigen Zeit den circadianen Rhythmus in der Zeit und der Amplitude verschieben kann [10]. Licht am späten Abend verzögert demnach die innere Uhr, da dem Körper signalisiert wird, es wäre noch Tag. Licht am frühen Morgen hingegen beschleunigt den Rhythmus. Analog zur Melatonin-Suppression konnte diese Lichtwirkung ebenfalls mit einer nächtlichen 6,5 stündigen vertikalen Lichtexposition mit weißem Licht¹ bei 100 lx am Auge nachgewiesen werden (Abbildung 33b) [1]. Geeignete Werte für die Praxis werden derzeit untersucht. Forscher halten es jedoch für möglich, dass bereits das Überschreiten einer Wirkungsschwelle von 30 lx am Auge über mehrere Tage hinweg für die Stabilisierung des circadianen Rhythmus ausreicht [11].

¹"Light was generated using overhead cool white fluorescent lamps (North American Philips Lighting, Bloomfield, NJ, USA) filtered with a Lexan 9030 UV restricting lens (General Electric Plastics, Pittsfield, MA, USA) and designed to provide uniform illuminance to the whole experimental room (Philips Lighting, The Netherlands). [6]"

Steigerung des Wachheitsgrades

Im Laufe eines Tages werden im menschlichen Körper unterschiedliche Hormone ausgeschüttet; morgens bei Tageslicht *Serotonin* und bei Dunkelheit am Abend *Melatonin*.

Das Hormon Serotonin wirkt stimmungsaufhellend und motivierend. Im Gegensatz zu Melatonin, welches den Menschen müde macht, verhilft Serotonin zu mehr Leistungshochs. Außerdem ist es sehr wichtig für die Melatonin-Produktion, da dieses in zwei Schritten aus der Aminosäure Tryptophan und Serotonin synthetisiert wird. Daraus kann gefolgert werden, dass genügend Serotonin am Tag die Melatonin-Ausschüttung in der Nacht positiv beeinflusst, wodurch ein tieferer und erholsamerer Schlaf gewährleistet werden kann.

Besonders in den Wintermonaten, in den Tagesrandstunden oder in schlecht ausgeleuchteten Räumen kann die Serotonin-Produktion gestört sein. Spezielle Lichttherapien oder Lichtduschen können die gezielte Ausschüttung von Serotonin bewirken und damit den Wachheitsgrad und die Leistungsfähigkeit steigern. Diese Konzepte sind in ihrem Spektrum und der Beleuchtungsstärke meist dem Tageslicht nachempfunden. Quellen belegen jedoch, dass ab etwa 100 lx Beleuchtungsstärke am Auge die subjektive Ermüdung sinkt bzw. die subjektive Munterkeit steigt [7] (Abbildung 35).

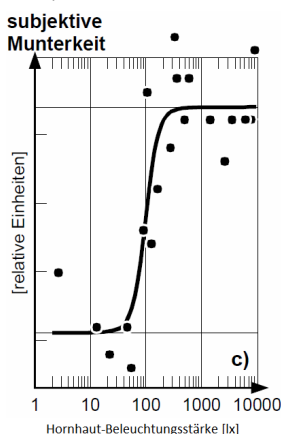


Figure 35: Subjektive Munterkeit [7].

Planungsempfehlungen

Auch die Lichtindustrie hat das Potenzial von melanopisch wirksamer Beleuchtung erkannt und erweitert dahingehend Ihr Produktportfolio. Die nächste Hürde besteht nun darin, diese Produkte korrekt einzusetzen, um auch die gewünschte

Wirkung zu erzielen.

Die Planung einer melanopisch wirksamen Beleuchtung ist sehr anspruchsvoll und kann nur mit Hilfe eines ganzheitlichen Licht- und Raumplanungskonzepts realisiert werden. Die nichtvisuelle Lichtwirkung hängt insbesondere vom Zusammenspiel der Faktoren Lichtspektrum, Beleuchtungsstärke, Lichtverteilung und Dynamik ab. Dementsprechend gilt für eine melanopisch wirksame Beleuchtung [2]:

- Lichtspektrum: Kurzwelliges blaues Licht (ideal: 450nm).
- Beleuchtungsstärke: Ab etwa 100 lx am Auge (Konkrete Werte werden noch erforscht).
- Lichtverteilung: Großflächig verteilt und von oben fallendes Licht, damit die melanopsinhaltigen Ganglienzellen im unteren und nasalen Bereich der Netzhaut erreicht werden.
- Dynamik: Zeitliche Änderungen des Spektrums, der Beleuchtungsstärke und der Lichtverteilung erhöhen die melanopische Lichtwirkung.

Es gilt: Das richtige Licht zum richtigen Zeitpunkt. Ein melanopisch wirksames Beleuchtungssystem muss sich an den circadianen Rhythmus und die individuellen Bedürfnisse des Nutzers anpassen.

Konkrete Planungsempfehlungen sind in der Norm DIN SPEC 67600 beschrieben. Dabei wird über die Gestaltung einer melanopisch wirksamen Beleuchtung für unterschiedliche Anwendungen (u.a. Pflegeheime, Ausbildungsstätte, Gesundheitseinrichtungen, Arbeitsplätze mit Schichtarbeit) informiert. Konkret empfiehlt die Norm für eine aktivierende Wirkung ein großflächig verteiltes Licht mit hohen Blauanteilen sowie einer Beleuchtungsstärke von 250 Lux bei 8.000 Kelvin Farbtemperatur [2]. Kritische Stimmen halten diese Werte jedoch für aus der Luft gegriffen und schwer umzusetzen.

Ein ganzheitliches Lichtkonzept für die Umsetzung in der Praxis ist beispielweise das Human Centric Lighting Konzept (HCL-Konzept) [12]. Dabei sorgen moderne Lichtquellen für das gezielte Lichtspektrum, Leuchten und Raumgestaltung für die Lichtverteilung und Lichtsteuerungssysteme für die Dynamik.

Das Angebot in diesem Bereich wächst. Lichtlösungen wie die Active Leuchten von TRILUX, Arktika-P Biolux von OSRAM sowie

komplette Beleuchtungssysteme wie das Heal-Well von Philips sind nur einige Beispiele der Produkte, die aktuell am Lichtmarkt für verschiedene Anwendungsbereiche angeboten werden. Auch namhafte Hersteller wie z.B. Waldmann, Zumtobel und Siteco arbeiten an vielversprechenden Konzepten. Bei all diesen Konzepten ist jedoch zu beachten, dass die zugrundeliegende melano-pische Lichtwirkung noch nicht vollständig erforscht und die resultierenden Wirkungen noch nicht abschließend belegt sind. Bis dato sind auch weiterhin Lichtlösungen, bei denen die melano-pische Lichtwirkung nicht miteinbezogen wird, Stand der Technik.

Bibliography

- [1] Schierz Ch.: Unspezifische biologische Lichtwirkungen am Arbeitsplatz. (2002)
- [2] Deutsches Institut für Normierung: Biologisch wirksame Beleuchtung - Planungsempfehlungen. DIN SPEC 67600, Berlin, Beuth Verlag (2013)
- [3] Lasko T.A., Kripke D.F., Elliot J.A.: Melatonin suppression by illumination of upper and lower visual fields. *J. Biol. Rhythms* V14 N2 (1999) P122-125.
- [4] Rimmer D.W., Boivin D.B., Shanahan T.L., Kronauer R.E. et al.: Dynamic resetting of the human circadian pacemaker by intermittent bright light. *Am. J. Physiol. Regulatory Integrative Comp. Physiol.* V279 (2000) P:R1574-R1579.
- [5] Visser E.K., Beersma D.G.M., Daan S.: Melatonin suppression by light in humans is maximal when the nasal part of the retina is illuminated. *J. Biol. Rhythms* V14 N2 (1999) P116-121.
- [6] Zeitzer J.M., Dijk D.-J., Kronauer R.E., Brown E.N., Czeisler C.A.: Sensitivity of the human circadian pacemaker to nocturnal light: melatonin phase resetting and suppression. *J. Physiol.* V526.3 (2000) P695-702.
- [7] Cajochen C., Zeitzer J.M., Czeisler C. A., Dijk D.-J.: Dose-response relationship for light intensity and ocular and electroencephalographic correlates of human alertness. *Behav. Brain Res.* V115 (2000) P75-83.
- [8] Wang J.Y., Hanifin J.P., Rollag M.D., Brainard G.C.: Ocular regulation of the human pineal gland: The significance of total retinal exposure for melatonin suppression. *Biologic Effects of Light 1998*, Kluwer Boston (1999) P367-373.
- [9] Gaddy J.R., Ruberg F.L., Brainard G.C., Rollag M.D.: Pupillary modulation of light-induced melatonin suppression. *Biologic effects of Light 1993*. W. de Gruyter, Berlin (1994) P159-168.
- [10] Jewett M.E., Rimmer D.W., Duffy J.F., Klerman E.B. et al.: Human circadian pacemaker is sensitive to light throughout subjective day without evidence of transients. *Am. J. Physiol. Regulatory Integrative Comp. Physiol.* V273 (1997) P:R1800-R1809.
- [11] Rosenthal N.E., Kasper S.F.: Licht-Therapie. Heyne Ratgeber Nr. 08/5150, 2. Auflage (1998).
- [12] Human Centric Lighting: By Stan Walerczyk, CLEP, LC, Principal, Lighting Wizards <http://humancentriclighting.com/wp-content/uploads/2012/07/Stan-Article-SSL1.pdf> (2015) (Abgerufen am 30.06.2015, 14:00)
- [13] Licht.wissen19: Wirkung des Lichts auf den Menschen http://www.licht.de/fileadmin/Publikationen_Downloads/1403_lw19_Wirkung_auf_Mensch_web.pdf (2014) (Abgerufen am 30.06.2015, 14:00)
- [14] Bieske K., Vandahl C., Schierz Ch.: Projekt "Licht und Gesundheit" - Feldstudie in Industriebetrieben https://www.tu-ilmenau.de/fileadmin/public/lichttechnik/Publikationen/2011/Bericht_Licht_und_Gesundheit_-Feldstudie_in_Industriebetrie.pdf (2011) (Abgerufen am 30.06.2015, 14:00)

Institut für Optische Systeme
Hochschule Konstanz
Brauneggerstr. 55
78462 Konstanz
www.ios.htwg-konstanz.de